The Dissertation Committee for Rahul R. Iyer
certifies that this is the approved version of the following dissertation:

Efficient Muscle Representation for Human Walking

Committee:

Dana Ballard, Supervisor

Don Fussell

Risto Miikkulainen

Luis Sentis

Peter Stone

Efficient Muscle Representation for Human Walking

by

Rahul R. Iyer, B.E.; M.S.

DISSERTATION

Presented to the Faculty of the Graduate School of

The University of Texas at Austin

in Partial Fulfillment

of the Requirements

for the Degree of

DOCTOR OF PHILOSOPHY

THE UNIVERSITY OF TEXAS AT AUSTIN

December 2012

Acknowledgments

It is difficult to overstate my gratitude to my mentor and supervisor, Dana Ballard. With his enthusiasm and his efforts to explain things clearly and simply, he helped to make undertaking research fun for me. Throughout my graduate research, he provided encouragement, sound advice, good teaching, and lots of great ideas. I would have been lost without his immense support.

I am also grateful to Mary Hayhoe, for keeping me grounded and providing sound advice on the practicalities of my research. I appreciate all the help and feedback from my peers and friends in the lab. I enjoyed discussing different aspects of motor control research with Dmitry, Joseph, and Leif. Further, feedback received from Gabe, Kat, Brian Sullivan, and Brian McCann has played an important part in molding my research work. I am obliged to all of them for providing insights and valuable ideas for my progress.

My special thanks go to the members of my dissertation committee - Peter Stone, Risto Miikkulainen, Don Fussell, and Luis Sentis - for their guidance and helpful discussions. I would also like to thank all of the staff members for their help in the last six years. From the UTCS department Katherine Utz, Gloria Ramirez, and Lydia Griffith have been prompt in helping me with numerous administrative issues. From the CPS department Christine Fry, Lou Montgomery, and Alice Goewey have been phenomenal with processing all my accounting and travel needs.

My parents, Ratna and Ramakrishnan Iyer, receive my deepest

gratitude and love for their endless dedication, support, and encouragement over the years without which it would not have been possible for me to come to the USA for graduate studies. I am indebted to them for inculcating in me the qualities of dedication and discipline. I thank my brother, Rohit, for showing me what it is to be a free spirit.

Above all, I would like to thank my wife, Sumegha, for her understanding and love during the past years. Her support and encouragement has seen me through tumultuous times and was in the end what made this dissertation possible.

This research work was funded in part by NIH grant EY019174 and NSF award IIS-0932277.

Rahul Iyer
Austin, December 2012

Efficient Muscle Representation for Human Walking

Publication No. _____

Rahul R. Iyer, Ph.D.
The University of Texas at Austin, 2012

Supervisor: Dana Ballard

Research in robotics has recently broadened its traditional focus on industrial applications to include natural, human-like systems. The human musculoskeletal system has over 600 muscles and 200 joint degrees-of-freedom that provide extraordinary flexibility in tailoring its overall configuration and dynamics to the demands of different tasks. The importance of understanding human movement has spurred efforts to build systems with similar capabilities and has led to the construction of actuators, such as pneumatic artificial muscles, that have properties similar to those of human muscles. However, muscles are far more complex than these robotic actuators and will require new control perspectives.

Specifying how to encode high degree-of-freedom muscle functions in order to recreate such movements in anthropomorphic robotic systems is an imposing challenge. This dissertation attempts to advance our understanding by modeling the workings of human muscles in a way that explains how the low temporal bandwidth control of the human brain could direct the high temporal

bandwidth requirements of the human movement system. We extend the motor primitives model, a popular strategy for human motor control, by coding a fixed library of movements such that their temporal codes are pre-computed and can be looked up and combined on demand. In this dissertation we develop primitives that lead to various smooth, natural human movements and obtain a sparse-code representation for muscle fiber length changes by applying Matching Pursuit on a *parameterized* representation of such movements. We employ accurate three-dimensional musculoskeletal models to simulate the lower body muscle fiber length changes for multiple repeatable movements captured from human subjects. We recreate the length changes and show that the signal can be economically encoded in terms of discrete movement elements. Each movement can thus be visualized as a sequence of coefficients for temporally displaced motor primitives.

The primary research contribution of describing movements as a compact code develops a clear hierarchy between the spinal cord and higher brain areas. The code has several other advantages. First, it provides an overview of how the elaborate computations in abstract motor control could be 'parcellated' into the brain's primary subsystems. Second, its parametric description could be used in the extension of learned movements to similar movements with different goals. Thirdly, the sensitivity of the parameters can allow the differentiation of very subtle variations in movement. This research lays the groundwork for understanding and developing further human motor control strategies and provides a mathematical framework for experimental research.

Table of Contents

List of Tables

List of Figures

List of Algorithms

Chapter 1

Introduction

A British neurologist, J. Hughlings Jackson (1835-1911), wrote: "the central nervous system knows nothing about muscles, it only knows movements" [Jackson, 1889]. The notion of 'movement', however, is undefined and implies an abstract representation of muscles. To generate purposeful behavior the central nervous system (CNS) has to coordinate the many degrees of freedom of the musculoskeletal system, taking into account the nonlinear characteristics of the muscles. Moreover, the same motor apparatus is used to achieve different goals in a variety of natural behaviors. A broad characterization of the neural control of movement at the systems level is still elusive as key issues remain unresolved. The basic representation of the somatosensory and motor areas has been challenged by micro-stimulation experiments in monkeys [Afshar et al., 2011; Graziano and Aflalo, 2007], the overall function of the cerebellum is still unsettled [Manto et al., 2011], and there is still an evolving understanding at a formal abstract level of how the cortical representations communicate with the elaborate reflex structure of the spinal cord [Pierrot-Deseilligny et al., 2005; Kiehn, 2005; Kiehn et al., 2010]. Our goal is to significantly advance the understanding of this interface by focusing on the abstract representations of signals that control human movement and respect basic musculoskeletal and neural constraints.

Previous research in motor control has tackled neural control with the

tools of classical mathematical optimization theory widely used in robotic models. Although small dynamical subsystems can be modeled with classical Newtonian equations [Todorov, 2004; Todorov et al., 2005; Buchli et al., 2011; Shadmehr and Mussa-Ivaldi, 2011], for mammalian systems with very high numbers of degrees of freedom, these equations prove prohibitively expensive to solve. Nonetheless, humans themselves are an existence proof that some kind of practical solution must exist, since they have exquisite motor coordination. At the same time, since their physical design is so specialized, one must be prepared that the human solutions might look very different than those dictated by the robotics-inspired classical approach.

Understanding human motor strategies is also beneficial to the robotics community. The technological breakthroughs of the last three decades in the areas of computer science and engineering, has immensely benefited robotics due to the fact that computationally demanding control, estimation, and machine learning algorithms can now be executed online and in real time. In particular, future robots will not only perform in industrial environments but they will also safely co-exist with humans in environments less structural and more dynamic and stochastic than the environment of today's factory. Despite all this evolution, learning for a robot how to autonomously perform human-like motor control tasks such as object manipulation, walking, running etc, remains an open problem. There is a combination of characteristics in humanoid bodies which is unique and it does not often exist in other cases of dynamical systems. These systems are usually high dimensional. Moreover their dynamical model is typically unknown and hard to estimate. In cases where a model is available, it is an approximation of the real dynamics, hampered by noisy and imperfect sensors.

All these characteristics of humanoid robots open the question of how humans resolve these issues due to the fact that they also perform motor control tasks in stochastic environments and deal with contact phenomena and sensor noise. Human muscles may span multiple joints, generally operating unlike torque generators, and their output (linear force) is said to be state-dependent (length being an example of state). The advantage of this complexity is to be able to configure oneself into various dynamical systems, and thus, have a large repertoire of configurations to bring to bear on many different kinds of tasks. The huge number of DOFs allows the system to solve motor coordination problems associated with mobility and manipulation in many different ways and enables it to adapt itself to different kinds of constrained environments. Furthermore, the human system has extensive passive compliance, allowing it to successfully interact with a range of objects with differing material and inertial properties. In addition, the human system is characterized by a higher strength-to-weight ratio, generally around 4:1 [van der Smagt et al., 2009, for review see]. The net result is, for adaptable, general-purpose motor behaviors, the human system is vastly superior to current robotic platforms.

Such physical advantages of the human body have led to concerted engineering efforts to replicate it in compliant and ambulatory systems like the Shadow Dextrous Robot Hand [sha], the BigDog Quadruped Robot [Raibert et al., 2008], and the PETMAN robot [Raibert]. The Pleated Pneumatic Muscle implemented in a humanoid at Vrije Universiteit Brussel [Vanderborght, 2007] and Electroactive Polymer (EAP) actuators [Bar-Cohen, 2000] are other examples of progress made in muscle-based approaches to robotic actuation. Furthermore, advances in cable driven technologies promise to allow additional

DOFs without prohibitive weight penalties. Such advances promise to move robotic technologies towards the superior levels of adaptability and control of the human system, but there are still many obstacles to overcome.

Planning movement trajectories for humanoid robots is often addressed by building a model to derive the input commands required to obtain a desired movement. Optimization is used in the case of redundancy to disambiguate between multiple solutions. However, in humanoid robots, the high redundancy and the large workspace of the system makes the search for a suitable plan challenging. Additional difficulties include time-varying environmental constraints and, for some applications such as bipedal walking, a limited time to find adequate solutions. An alternative approach is to study the human system as a model that anticipates emerging developments in robotic technology including creation of advanced muscle-like systems. Even though the human body is highly flexible there are some limitations to it. Among its apparent imperfections are the sluggish actuators (the muscles), the confusing sensors (noisy proprioception), and the long-time delays in all the pathways that are used to deliver control signals to the muscles and sensory information to the controller. The low temporal bandwidth and high latency of the human system implies that it has to make extensive use of feedforward models that predict the outcomes of movements. As a consequence the human system must choose pre-programmed set movements in advance. One way this could be done is to access a movement library, and this thesis shows how to discover and encode such a library from actual human movement distribution.

Indeed, it seems that, in animals, the planning of the task to be performed is decoupled from the actual trajectory generation (i.e., the temporal sequence of activation of the muscles). More precisely, neurally

encoded movements motor primitives have been brought to light in the spinal cord in various animals [Bizzi et al., 2008; Grillner, 2006], indicating that (high-level) trajectory planning in animals could come down to the selection and the appropriate activation of pre-existing motor primitives. Any action can be built of a number of motor primitives recruited with corresponding scaling coefficients.

In this dissertation, we define specific motor primitives - also called 'basis functions' in signal processing - that encode the temporal history of muscle fiber lengths from measured movements of the human subjects, with the objective of creating new movements in terms of linear variations of the codes parameters. The muscle fiber length histories can be thought of as motor basis functions that allow general movements to be described as a weighted sum of basis functions. Thus many different movements can be simply described in terms of different basis function weightings. The central component of the thesis describes the use of multi-scaled Gabor motor primitives to code muscle length changes over time. Mallat and Zhang [1993] introduced a general method, called *Matching Pursuit*, for approximate decomposition that iteratively computes a sparse solution. They also discuss a faster, discrete implementation for an overcomplete dictionary of multi-scale Gabor time-frequency atoms. We extend this technique by allowing the dictionary atoms to update themselves to a better Gabor atom in a local neighborhood during the decomposition process. This allows us to decompose the signals using a smaller dictionary, albeit one that is customized to the data. Our new form of parametric updates in Matching Pursuit ensures that the dictionary atoms reflect the data, but still maintain the smooth nature of a Gabor which would be lost in the case of applying arbitrary task space updates.

In the study of human movements, an established notion is that movements are graceful and smooth [Sejnowski, 1998]. We hypothesize that the brain reduces the complexity of controlling an extremely under-constrained limb by representing its smooth, natural movements in smaller chunks, or elements, of basis functions. It has been suggested that the primary visual cortex [Olshausen and Field, 1996] and the auditory system [Smith and Lewicki, 2006], encode their signals using a sparse representation with the help of an overcomplete dictionary or bases. We extend this representational strategy to motor primitives by performing a global analysis of the muscle length signal and study the performance of sparse-encoding on natural body movements. In this thesis we hypothesize that reducing a movement signal to a small set of coefficients would not only be efficient but enable easier learning, control, and classification. Our approach is a significant advance with respect to previous abstract models in that it shows how to encode the elaborate temporal signals in the spinal cord into a compact time-invariant code that potentially can be exploited by the cerebellum and forebrain. This code is compatible with recent cortical recordings [Afshar et al., 2011], requires very low bandwidth to communicate, employs muscle synergies, and makes central use of spinal cord pattern generators.

1.1 Thesis contributions

This thesis specifically aims to answer the following question:

> How can we learn an efficient muscle representation for rhythmic human movements from demonstration data?

Our basic movement code is inspired by advances in the understanding of perceptual codes in early cortex. In both visual [Olshausen and Field, 1997; Rao and Ballard, 1998] and auditory spaces [Smith and Lewicki, 2006], it has been recognized that ecologically significant stimuli comprise a very small fraction of the representable stimuli. This has allowed cortical neuron's receptive fields to be interpreted as *sparse codes*. In a similar manner, we posit that the temporal signals in spinal cord pattern generators can be seen as a a basis for sparse code for movements. Thus general temporal signals used in posture changes can be thought of as composable in terms of a weighted sum of primitive pattern generator outputs, or mathematically termed as *temporal basis functions*.

The basis function decomposition technique represents a signal as a superposition of waveforms. Other than the Fourier representation of sinusoids, other representations include Wavelets, Gabor, Cosine and Wavelet packets, Chirplets, and a wide range of other dictionaries. Although dozens of similar interesting dictionaries have been proposed over the last few years, we focus in this document on a multi-scale Gabor dictionary as a means to decompose signals in both time and frequency space. The primary motivations for doing this are as follows.

1. Human movements can be decomposed into time limited temporal segments owing to changing phasing and contact relationships.

2. Human movements, owing to inertia, tend to have a temporal smoothness that can be approximated nicely with sinusoids of varying frequencies.

3. The reduced bandwidth required to drive the movement allows for abstract control strategies.

In summary, the contributions of the dissertation are given below.

1. **Extracting motor primitives for muscle signals using natural human movements.** This dissertation provides evidence supporting efficient coding theory as a general computational principle in motor control and extends previous work on motor primitives by providing a mathematical framework for learning and encoding primitives. We present a novel algorithm that takes advantage of parametric formulation of primitives. Our solution extends other sparse encoding systems by not only producing a minimal encoding set, but also minimizes the stored primitive dictionary.

2. **Parametrized dictionary of motor basis functions.** The research presented in this dissertation expands upon the existing models of efficient coding and addresses a fundamental problem of high-dimensionality in representation using sparse-coding. There have been notable success in using independent components analysis to understand coding in primary visual cortex and auditory nerve tuning. This document provides a parametric approach to apply these techniques to encapsulate various rhythmic movements and efficiently recreate those movements. We present detailed analysis of movements produced using an efficient code of a superposition of Gabor functions.

3. **Synergistic coding of movements to correlate muscles in synergy.** Synergy has been proposed as a neural mechanism that ensures task-specific co-variation of control variables providing for desired stability properties of an important output variable. The dissertation

demonstrates this correlation between the encoding of synergistic muscles during walking movements and provides further improvement in efficiency by employing the synergy.

4. **Generalization of learned primitives using Jacobian.** Applying parameterized sparse coding provides a representation framework for movements. To correlate this representation with goals in task-space a Jacobian structure can be employed that translates changes in muscles to specific changes in the end-effector. This research work provides this simple technique as a framework to generalize new movements from learned basis functions. We conduct a pilot study to show the viability of the method.

1.2 Thesis overview

Chapter 2 gives a brief overview of past studies to understand human motor control and the origin of motor primitives. The chapter aims to introduce the reader to the concepts that play an important role in this thesis.

In chapter 3 we begin to address the problem of efficient coding and solutions that provide highly efficient representations of time-varying signals for a given dictionary. Further, we use our theoretical model for learning efficient codes to learn a dictionary adapted to the statistics of movement data. The chapter finally introduces a novel approach to parametrize these sparse coding technique.

Chapter 4 delves into the methodology employed in this research work and presents results of applying sparse encoding techniques to motion capture and muscle data. The chapter includes a detailed description of all the

equipment and experimental procedures used for capturing the movements.

Chapter 5 delineates the idea of synergies and presents results for extending the encoding scheme for synergistic movements. We also briefly discuss the viability of applying a Jacobian analysis to generalize a pre-learned movement.

Finally, chapter 6 discusses research work by other scholars covering areas of optimal motor control and perspectives about involvement of spinal cord in human movement. Chapter 7 summarizes the usefulness of this research and potential areas for extending the work.

Chapter 2

Background and Context

The aim of this research is to develop a framework for learning motor primitives for locomotion movements in high degree-of-freedom (DOFs) bodies from demonstration data. This problem is still open and challenging, notably because planning complex, multidimensional trajectories in time-varying environments is a laborious and costly process. In addition, while efficient controllers for following predefined trajectories have been designed, building an efficient mechanism to produce these trajectories is still an open problem.

This chapter sets the context for the remainder of the thesis. We begin with a review of previous research on motor primitives in robotic systems. These systems give a higher level movement strategy, without enforcing a mechanism for translation to muscle signals. We follow that with the origin of motor primitives in animal and human studies, motivating the need for this research work.

2.1 Robotic Bipedal Locomotion

There are two main approaches to robotic locomotion: model-based approaches for slow locomotion on challenging terrain and CPG-based approaches for fast locomotion with possible change in gaits. We briefly present

these two approaches.

2.1.1 Model-based approaches

Traditional approach towards bipedal locomotion has focused on the control of balance. Several criteria have been developed to characterize stability, but they provide sufficient not necessary conditions and thus constrain the space of possible stable walking trajectories. They do not provide by themselves solutions to the stability problem.

Popular criteria used in the literature are Zero moment point (ZMP), first discussed by Elftman [1938] for the study of human biomechanics, and the Centroidal moment pivot (CMP) [see Popovic et al., 2005, for review] ZMP is defined as the point on the ground surface about which the horizontal component of the moment of ground reaction force is zero [Arakawa and Fukuda, 1937]. To ensure stability, this point should never leave the convex hull defined by the contact points. In addition the ZMP criterion hold only in cases where the contact points are in the same plane. Centroidal moment pivot, a generalization of ZMP, is the point on the foot/ground surface of a robot where the total ground reaction force would have to act such that its centroidal angular momentum stays constant. Impressive results based on a model-based approach include the work with the Asimo robot by Honda.

2.1.2 CPGs-based approaches

In biology, a fundamental notion for the generation of rhythmic movements is central pattern generators (CPGs) [see Grillner, 2006, for review].

Central pattern generators (CPGs) are neural circuits found in both

invertebrate and vertebrate animals that can produce rhythmic patterns of neural activity without receiving rhythmic inputs. For example, the recruitment of different CPGs enables a newborn chicken to perform appropriate hatching movements to break the eggshell and to stand, walk on two legs, breathe, and to perform appropriate neck and eye movements [Grillner, 2006].

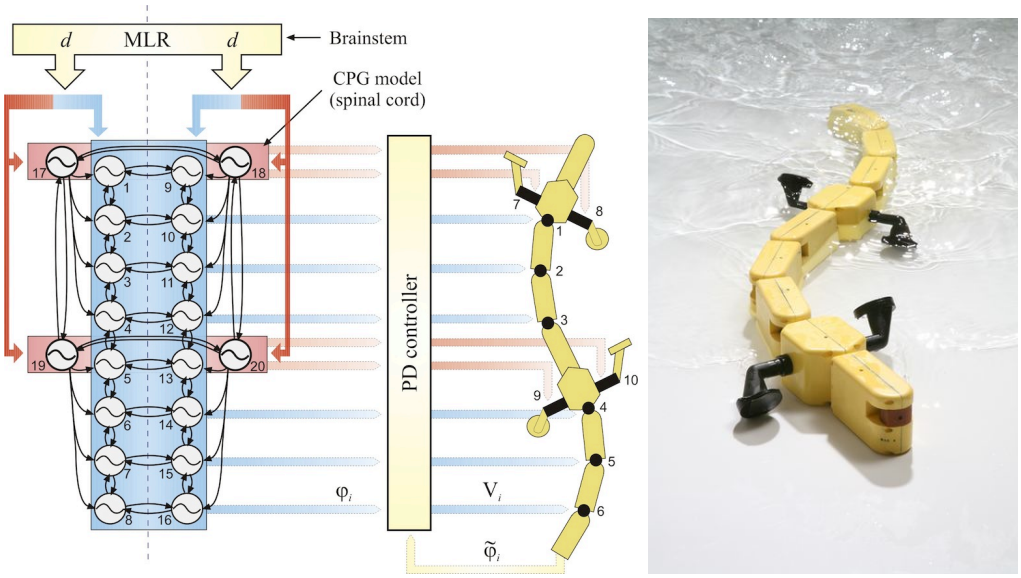

Figure 2.1: CPG model applied on a Salamander-like robot. Phase oscillators controlled by a drive signal were used in conjunction with Proportional-Derivative (PD) feedback controllers to drive joint motors. Technical Figure by A. Ijspeert and Photograph by A. Herzog, courtesy Biorobotics Laboratory, EPFL [Ijspeert et al., 2007])

This concept is interesting for modeling locomotion because it simplifies the high-level control, but also because the gait can be intrinsically defined in the CPG network. Ijspeert [2008] has shown how simple CPG oscillators can be used to develop efficient controllers for a salamander-like robotic locomotion (Figure 2.1). The central idea behind the model is that salamander bi-modal locomotion can be explained by adding limb oscillatory centers with lower

intrinsic frequencies and lower saturation frequencies to a lamprey swimming circuit.

Both the model-based approach and the CPG-based approach have their pros and cons: on the one hand, CPGs restrict the system to the oscillate only in the frequencies present in the system, thus losing flexibility, while it is difficult to modulate the policies obtained according to the ZMP fast enough, e..g to deal with model mismatch.

It is not inconceivable to think that both approaches can exist in the same control system. In this dissertation, however, we will be focusing on the CPG approach.

2.2 Motor Primitives

The spinal cord is typically viewed as a relatively simple structure with little cognitive abilities, and is mostly credited with unsophisticated reflexes. From a movement perspective, however, the spinal cord has been shown to be vitally important. To understand the complexities of movements, let us consider a simple task of moving the tip of the index finger from some initial position to some final position. The solution is clearly not unique with a number of possible trajectories that could achieve this goal. Even after a solution is chosen, its implementation can be achieved by multiple combinations of joint motions at shoulder, elbow, and wrist. Solving this "inverse" problem of computing the control signal that produces a movement is a hard computational challenge because of the need to coordinate several limb segments, and the continuous changes in the mechanical properties of the limbs and the environment with which they come into contact.

It has been suggested that one possible solution to this complex problem is using pre-learned movements or primitives. A number of studies of motor learning have lent support to the idea that the central nervous system creates, updates and exploits internal representation of limb dynamics to deal with the complexity of inverse dynamics. There is evidence that such internal representations are probably built by combining modular primitives as well as other building blocks found in higher structures [Bizzi et al., 2000].

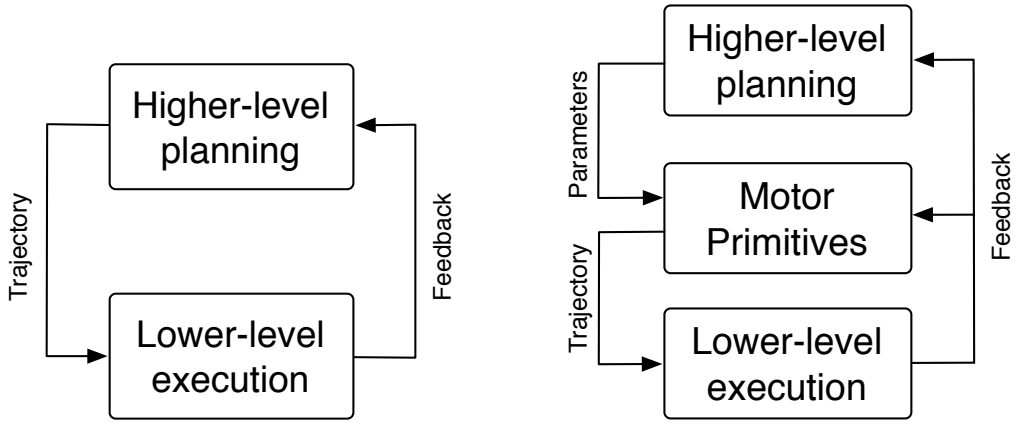

(a) Traditional approach (b) Motor Primitives approach

Figure 2.2: Contribution of motor primitives for motor control. a) In the traditional approach, a planner computes the motor commands and controls the system using feedback control. b) In motor primitives approach, there exists two levels of feedback. A short feedback loop is used to modulate the plant using an oscillator (or primitive), and a long feedback loop enables the higher-level controller to regulate the parameters of the primitive to achieve a planned goal.

Figure 2.2 illustrates the contribution of motor primitives. In the traditional approach, there are usually two different processes: a high-level planner that computes the desired trajectories and a low-level controller (e.g., a PID controller) that transforms the desired trajectories into motor commands,

generally based on the error between the current states and the desired state. In the case of motor primitives we add a middle-level controller to the system that is composed of a set of trajectories with predefined dynamics. In terms of robotic control, the motor primitives can thus be seen as sophisticated low-level controllers, in which a priori knowledge about the movements to be performed is embedded and that can be modulated according to feedback information. The advantage of using these primitives is threefold. First, they ease the planning problem by reducing the workspace of the robot through the constraint of the dynamics of the motor primitives. Second, they provide the system with a fast, low-level feedback loop that can be used to rapidly correct trajectories according to the incoming sensory information if required (without the need for a new motor plan). Finally, different degrees of freedom can be coupled together to ensure inherent synchronization and coordinated behaviors. In other terms, motor primitives provide an effective, dynamic way to embed a priori knowledge about the task into the low-level control system.

2.2.1 Motor Primitives in Animals Studies

Motor primitives have been shown to be present in various spinalized animal studies [Mussa-Ivaldi et al., 1994] and have also been suggested in humans based on observations in patients with a severe spinal cord injury [Shapkova, 2004]. One of the remarkable discoveries includes study of the wiping reflex in decapitated frogs. If an experimenter places a stimulus (a small piece of paper soaked in a weak acid solution) on the back of a sitting spinal frog, the frog, after a certain latent period, performs a series of finely coordinated movements wiping the stimulus from the back and, sometimes, throwing it away from the body. The joints of the hindlimb share the task

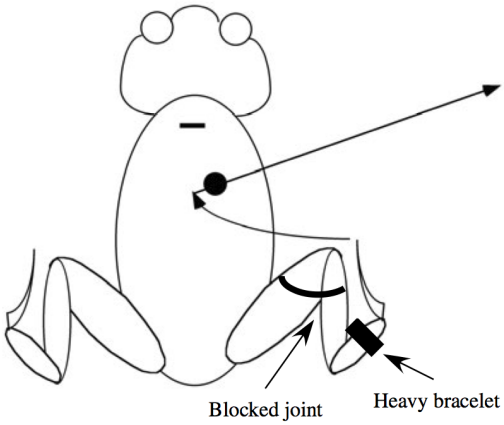

Figure 2.3: The spinalized frog was able to perform accurate wiping in conditions of loading of a distal leg segment with a heavy bracelet and in conditions of blocking motion in one of the major joints (knee joint).

and show reproducible patterns of their trajectories. There are a number of unique attractive features in this type of reflex behavior: First, since the animal is spinal, there is no influence of a neural inflow (no intention). Second, the wiping movement is stimulus-directed (goal-based), reproducible, and can easily be evoked. Third, it is a multi-joint movement performed by a kinematically redundant effector: There are four major joints in the frog's hindlimb, even if one ignores joints of the toes and whole-body movements. To understand how the limbs produce such movements, a series of experiments studied the effects of unexpected perturbations on the wiping patterns. In one of the experiments, either a loose thread was placed on the hindlimb, or a cast was placed on one of the joints (Figure 2.3). In each case, the frog was able to wipe the stimulus accurately. In experiments with joint fixation, the frog used the multi-joint design of the limb to compensate the unexpected errors introduced by the restrained joint. If one of the joints of the hindlimb is blocked

(with a loop or with a splint), other joints modify their action such that the toes get to the target area and perform accurate wiping movements [reviewed in Latash, 1993].

The frog experiments indicate an important finding: the spinal cord performed error correction. Apparently, the frog's spinal cord generates the wiping actions without any help from the brain because the two portions of the CNS cannot exchange signals. Each action represents a complex, multi-joint, multi-muscle action. For a single location of a stimulus, actions within a series of wiping movements are quite different. In particular, the toes that wipe the stimulus off the skin perform the quick wiping motion in different directions, with different attack angles. In different wiping actions and in different conditions, the frog repeats performing the task of wiping the stimulus off its body with non-repetitive, flexible motor patterns. To test the neurophysiological basis of the frog hindlimb movements, a group from MIT led by Emilio Bizzi measured the effects of electrical stimulation applied directly to structures within the spinal cord on hindlimb endpoint action [Bizzi et al., 1995; Mussa-Ivaldi et al., 1994]. Stimulation at a mid-thoracic level led in most cases to a hindlimb motion to a new position or, less frequently, to an anatomically extreme posture. These experiments resulted in force maps, families of force vectors produced by a standard stimulation applied when the limb was held at different spatial locations. All the force fields could be classified as belonging to three groups, converging to a point in space, forming a circular pattern about a point in space, and leading in a certain direction. Further modeling [Giszter et al., 1993] has shown that the set of three groups of force fields is sufficient to generate any arbitrary force field that may be necessary to produce any endpoint action. The force fields

produced by electrical stimulation of the frog spinal cord showed effects of linear superposition.

These studies culminated in an idea of the spinal cord containing motor primitives, that is, neural structures producing relatively simple blocks for complex actions. Any action is built of a number of motor primitives recruited with corresponding scaling coefficients. Similar to the frog experiments, if the paws of a spinal cat are placed on a treadmill, movement of the treadmill at a constant speed can induce stepping of the limbs with a coordinated motion of individual limbs typical of a gait. Changing the speed of the treadmill leads to changes in the stepping frequency, and when the speed reaches a certain threshold, the gait changes from walking to trotting and to galloping. The possibility of such a change in gait without explicit commands from the brain indicates spinal cord structures driven by the reflexes triggered by external stimulus.

The upshot is that evidence from human and other animal experiments suggest motor primitives as the basis for volitional motor control. The notion of motor primitives is appealing, because it does not rely on inverse dynamics computations to generate the appropriate joint torques for a given trajectory. Given that the equations of motion for inverse dynamics computations of multi-joint movements are very complex, avoiding such calculations potentially reduces the computational load of the control system.

2.3 Summary

The traditional approach for robotic/humanoid locomotion is to plan trajectories that can be executed using optimal controllers. An alternative approach is to replicate the (vertebrate) locomotor system which is organized

such that the spinal CPGs are responsible for producing the basic rhythmic patterns, and that higher-level centers are responsible for modulating these patterns according to environmental conditions. Such a distributed organization presents several interesting features. Firstly, it enables fast reaction times by providing short feedback loops between lower-level controllers (muscles) and intermediate-primitives layer (spinal cord). Second, it dramatically reduces the dimensionality of the space in which higher-level controllers need to search for an optimal solution. Indeed the control signals in general do not need to specify muscle activity but only modulate CPG activity. Finally, due to the reduced dimensionality, the maximum necessary bandwidth between higher-level planners and lower-level controllers is reduced.

Chapter 3

Efficient Coding Theory

The previous chapter introduced the notion of motor primitives and the need to represent the dynamics of natural movements using real-valued functions. In previous studies, it has been recognized that ecologically significant stimuli comprise a very small fraction of the representable stimuli. This has allowed cortical neurons' receptive fields to be interpreted as *sparse codes*. This chapter gives an overview of how such efficient coding theories can be used to learn an appropriate basis function representations. We begin with a tour of sparse coding theories with a focus on a particular algorithm, Matching Pursuit. We follow that with the primary contribution of this thesis - a parametric approach to matching pursuit.

3.1 Introduction

Sparse representations of signals have received a great deal of attentions in recent years. The problem solved by the sparse representation is to search for the most compact representation of a signal in terms of linear combination of atoms in an overcomplete dictionary. Olshausen and Field [1996] showed that when a sparse, independent code is sought for time-varying natural images, the basis functions that emerge resemble the receptive field properties of cortical simple-cells in both space and time. Moreover, the model yields a representation of time-varying images in terms of sparse, spike-like events.

It is suggested that the spike trains of sensory neurons essentially serve as a sparse code in time, which in turn forms a more efficient and meaningful representation of image structure. Thus, a single principle may be able to account for both the receptive properties of neurons and the spiking nature of neural activity.

Smith and Lewicki [2006] showed that, for natural sounds, the complete acoustic waveform can be represented efficiently with a nonlinear model based on a population spike code. In their model, idealized spikes encode the precise temporal positions and magnitudes of underlying acoustic features. They find that when the features are optimized for coding either natural sounds or speech, they show striking similarities to time-domain cochlear filter estimates, have a frequency-bandwidth dependence similar to that of auditory nerve fibers, and yield significantly greater coding efficiency than conventional signal representations. These results indicate that the auditory code might approach an information theoretic optimum and that the acoustic structure of speech might be adapted to the coding capacity of the mammalian auditory system. Olshausen and Field [1996] and Smith and Lewicki [2006] presented evidence supporting efficient coding theory as a general computational principle in human perception. Our goal with this thesis, is to extend this information theory principle to apply to motor commands and to exhibit evidence for efficient coding for movements.

Using motor or movement primitives to produce a required real-valued signal by superposition can be an efficient way to encode a high-dimensional data space. Such representations can be constructed by decomposing signals over elementary waveforms chosen in a family called a *dictionary*. An orthogonal basis is a dictionary of minimum size that can yield a sparse

representation if designed to concentrate the signal energy over a set of few vectors. Bases such as the Fourier or wavelet can provide a useful representation of some signals, but they are limited because they are not specialized for the signals under consideration.

An alternative and potentially more general method of signal representation uses so-called overcomplete bases (also called overcomplete dictionaries), which allow a greater number of basis functions (also called dictionary elements) than samples in the input signal. Under an overcomplete basis, the decomposition of a signal is not unique, but this can offer some advantages. One is that there is greater flexibility in capturing structure in the data. Instead of a small set of general basis functions, there is a larger set of more specialized basis functions such that relatively few are required to represent any particular signal. These can form more compact representations, because each basis function can describe a significant amount of structure in the data. For example, if a signal is largely sinusoidal, it will have a compact representation in a Fourier basis. Similarly, a signal composed of chirps is naturally represented in a chirp basis. Combining both of these bases into a single overcomplete basis would allow compact representations for both types of signals [Mallat and Zhang, 1993; Chen et al., 1999].

Assuming the terminology in [Chen et al., 1999], a signal $x(t) \in \mathbb{R}^n$ can be encoded with a collection of parametrized waveforms, called a dictionary, $D = \phi_\gamma, \gamma \in \Gamma$ as,

$$x(t) = \sum_{\gamma \in \Gamma} \alpha_\gamma \, \phi_\gamma(t) + R^{(M)}, \tag{3.1}$$

where $R^{(M)}$ is residual signal in the case of an approximate decomposition. The waveforms ϕ_γ are discrete-time signals of length n, called as *atoms*. Depending

on the dictionary, parameter γ can have the interpretation of indexing frequency (Fourier representation), of indexing time/scale jointly (Wavelet dictionaries), or of indexing time/frequency jointly (Gabor dictionaries). Usually dictionaries are complete or overcomplete, in which case they contain exactly n atoms or more than n atoms, but one could also have continuum dictionaries containing an infinity of atoms and under-complete dictionaries for special purposes, containing fewer than n atoms.

3.2 Encoding algorithms

Finding an optimal decomposition of waveforms is an NP-hard problem [Davis, 1994], but the problem is made simpler by solving for an approximate decomposition. To do this, overcomplete dictionaries are used as they provide greater flexibility in capturing the data. Instead of a small set of general basis functions, there is a larger set of more specialized basis functions such that relatively few are required to represent any particular signal. A sparse representation is a result of the presence of specialized basis functions that closely resemble the decomposed signal. Further, pursuit algorithms reduce the computational complexity by searching for efficient but non-optimal approximations. One such algorithm is the matching pursuit, which reduces the computational complexity with a greedy strategy.

3.2.1 Matching Pursuit

Matching pursuit, introduced by Mallat and Zhang [1993], is a greedy algorithm that computes a good suboptimal approximation of a signal $x(t)$ using successive orthogonal projections onto dictionary elements. The

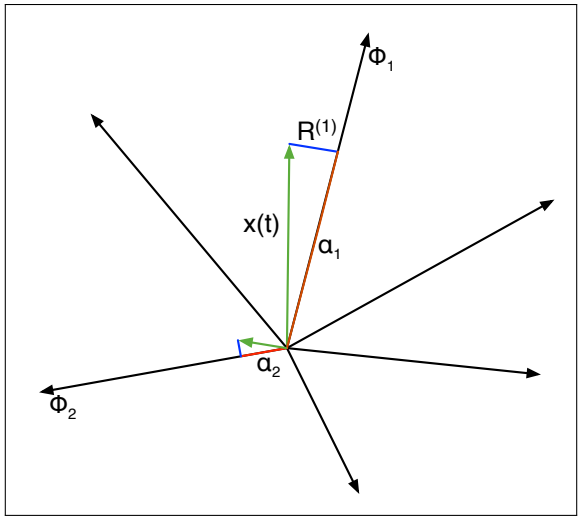

Figure 3.1: Geometrical illustration of the Matching Pursuit algorithm.

algorithm picks the vector $\phi_{\gamma_i} \in D$ for each iteration such that,

$$\phi_{\gamma_i} = \underset{\phi_\gamma \in D}{\operatorname{argmax}} \left| \left\langle R^{(i)}, \phi_\gamma \right\rangle \right|$$

where $R^{(i)}$ is the residual approximation error.

We start as,

$$R^{(1)} = R^{(0)} - \left\langle R^{(0)}, \phi_{\gamma_0} \right\rangle \phi_{\gamma_0}, \quad \text{and} \tag{3.2}$$

$$R^{(0)} = x(t). \tag{3.3}$$

The process continues in the next iteration by approximating the residue $R^{(2)}$ by selecting another best vector ϕ_{γ_1} from the dictionary. After M iterations the final signal decomposition will be

$$x(t) = \sum_{m=0}^{M-1} \left\langle R^{(m)}, \phi_{\gamma_m} \right\rangle \phi_{\gamma_m} + R^{(M)}.$$

Since each residual vector $R^{(i)}$ is orthogonal to the corresponding best vector ϕ_{γ_i}, we get an energy conservation equation

$$||x(t)||^2 = \sum_{m=0}^{M-1} \left|\left\langle R^{(m)}, \phi_{\gamma_m} \right\rangle\right|^2 + \left|\left|R^{(M)}\right|\right|^2.$$

The decoding algorithm minimizes the l^2 norm of the coefficients of the decomposed basis functions. Figure 3.1 provides a geometrical interpretation of the algorithm, where the signal $x(t)$ is projected onto the first basis function ϕ_1 (in this case, the basis functions are labeled in order of projection, but this is not the case for a generalized situation), producing a residual $R^{(1)}$, which becomes the signal for the next iteration.

Data: $X(t)$: Input signal ;
M: Number of basis functions combined in each encoding;
Result: $\alpha_{\gamma_i}, i = 1 \ldots M$: Sparse encoding for each input
while *global reconstruction error* $<$ *threshold* **do**
  for $x \in X$ **do**
    Initialize $R = x$;
    for $i \leftarrow 1$ **to** M **do**
      Project R onto dictionary, pick max atom ϕ_{γ_i};
      Compute $\alpha_{\gamma_i} = \langle R, \phi_{\gamma_i} \rangle$;
      Add α_{γ_i} in current input solution ;
      $R = R - \alpha_{\gamma_i} \phi_{\gamma_i}$;
    end
  end
end

Algorithm 1: Matching Pursuit

This is, however, optimized to the current dictionary. To adapt the dictionary to the data, the winning basis function in every iteration is partially moved towards the input signal in that iteration by adding the residual signal

to it. Thus the update step for iteration i will be $\phi_{\gamma_i} := \phi_{\gamma_i} + \beta R^{(i+1)}$, where β is a diminishing learning rate. During learning, each function ϕ_i would be rotated by a positive factor, towards the projected signal in the ith iteration.

3.2.2 Probabilistic Matching Pursuit

Probabilistic matching pursuit is a randomization of the matching pursuit algorithm where dictionary elements are selected at random from a list of promising candidates (those above a certain threshold inner product). The intuition behind picking an element at random is to ensure that we don't lose flexibility by always picking the "best" dictionary atom. Random expansions do not force us to restrict searches to a fixed subset of the dictionary and permits us to improve results by averaging. The modification is as follows: at each time step, a dictionary atom is selected randomly from the distribution with probability,

$$P(\alpha_i = \alpha_{\gamma_i}) = \frac{\Theta(\alpha_{\gamma_i}) e^{\eta \alpha_{\gamma_i}}}{Z(\eta, \alpha_{\gamma_i})},$$

where γ_i is the index of the unit to be chosen in the ith iteration and α is the coefficient of the chosen unit. $\Theta(x)$ is the Heaviside function, η^{-1} is a temperature parameter, and Z is a normalizing term given by:

$$Z(\eta, \alpha_{\gamma_i}) = \sum_{\gamma} \Theta(\alpha_{\gamma_i}) e^{\eta \alpha_{\gamma_i}}$$

Thus, the probability with which a unit is selected increases when its response coefficient is higher, i.e. it better predicts the input. The temperature parameter allows us to maintain the randomness of the selection and is typically annealed as the learning improves, resulting in the deterministic form of the algorithm at the end.

3.3 Model

3.3.1 Overcomplete Dictionary

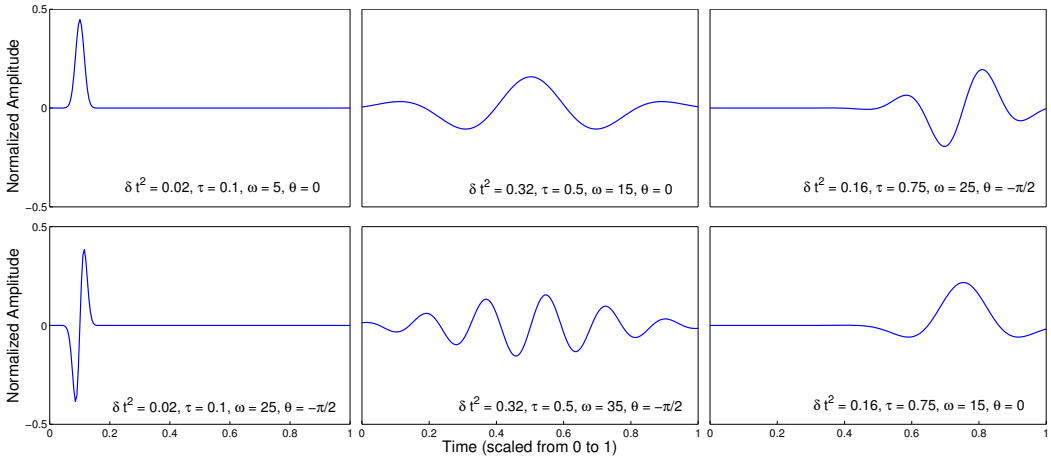

Figure 3.2: Multi-scale Gabor dictionary atoms across time. Scale, frequency, time shift, and phase are the four variable parameters. Shown here are example atoms of the initial dictionary with time scaled from 0 to 1, where 0 is start of movement, and 1 indicates end of movement.

The basis function decomposition technique represents a signal as a superposition of waveforms. Other than the Fourier representation of sinusoids, other representations include Wavelets, Gabor, Cosine and Wavelet packets, Chirplets, and a wide range of other dictionaries. Although dozens of similar interesting dictionaries have been proposed over the last few years, we focus in this document on a multi-scale Gabor dictionary as a means to decompose signals in both time and frequency space. The primary motivations for doing this are as follows.

1. Human movements can be decomposed into time limited temporal segments owing to changing phasing and contact relationships.

2. Human movements, owing to inertia, tend to have a temporal smoothness that can be approximated nicely with sinusoids of varying frequencies.

3. The reduced bandwidth required to drive the movement allows for abstract control strategies.

As described by Chen et al. [1999], the Gabor dictionary is given as $\gamma = (\omega, \tau, \theta, \delta t)$, where $\omega \in [0, \pi)$ represents the frequency, τ represents the location in time, θ is a phase, and δt is the duration. The atoms of the dictionary are defined as,

$$\phi_\gamma(t) = e^{\frac{-(t-\tau)^2}{\delta t^2}} cos\,(\omega(t-\tau)+\theta).$$

For fixed δt and $\theta \in \{0, \pi/2\}$, a discrete Gabor dictionary would be complete for $\omega_k = k\Delta\omega$ and $\tau_l = l\Delta\tau$, for sufficiently fine $\Delta\omega$ and $\Delta\tau$ (see [Chen et al., 1999; Daubechies, 1988]), where k and l are integers. For our purposes, we would like the dictionary to be adapted by the learning algorithm so that it spans the space of movement signals in the data. To initialize the dictionary, we set $\Delta\tau$ as a multiple (l) of the sampling rate of the signal, and $\Delta\omega = 3$, resulting in a sufficient resolution in the frequency space.

Figure 3.2 illustrates example atoms of the Gabor dictionary used in this paper. The wavelets were initialized with dyadic scales, starting from a scale that still retains the smoothness of the Gabor (e.g. first column of figure 3.2), and ending in a scale that enables the Gabor to extend to the whole movement span (e.g. second column of figure 3.2). The exact structure of the dictionary at any time, however, would be determined by the learning algorithm, described in Section 3.3.2. Although each dictionary atom is active only at a specific time, it is defined for the entire movement time (zero for

the non-active part), to easily enable a scaled superposition of different atoms when reproducing a movement signal.

3.3.2 Parametric Matching Pursuit

As described in Section 3.2, in matching pursuit, the winning basis function in every iteration is partially moved towards the input signal in that iteration by adding the residual signal to it. Thus the update step for iteration i will be $\phi_{\gamma_i} := \phi_{\gamma_i} + \beta R^{(i+1)}$, where β is a diminishing learning rate. It is important to note that such an update would not maintain the parametric form of the dictionary. Hence, we update the chosen dictionary atom in each iteration by employing a single-step search in the local neighborhood of the parameters of the chosen atom. This leads to the update rule $\gamma_i := \gamma_i + \alpha\bar{\gamma_i}$, where

$$\bar{\gamma_i} = \underset{\gamma' \in \Gamma'}{\operatorname{argmax}} \left| \langle x(t), \phi_{\gamma'} \rangle \right|.$$

γ' is defined as the set all parameters that are one stepsize from γ_i. A single step in each dimension k of the parameter space is defined as,

$$\delta E^k_{\gamma_i} = \frac{\left|\left| R^{(i)} \right|\right|}{\langle x(t), x(t) \rangle} \epsilon^k, \text{where}$$

ϵ^k is set as half of the maximum range of the parameter. The combined single step δE_{γ_i} is defined as all combinations of single steps $\pm\delta E^k_{\gamma_i}$. The intuition behind the single step search is that if the norm of the residual $R^{(i)}$, is close to the maximum value, $\langle x(t), x(t) \rangle$, then the stepsize becomes close to half of maximum value of the parameter. This would imply a big search step since the residual is high. On the contrary, if residual is small, the search is restricted to the immediate neighborhood of γ_i.

Data: $X(t)$: Muscle length trajectories for all muscles
Result: D: Dictionary for sparse encoding
Initialize parameters evenly in pre-defined range ;
Create Gabor dictionary for parameters;
while *global reconstruction error* $<$ *threshold* **do**
    for $x \in X$ **do**
        Initialize $R = x$;
        for $i \leftarrow 1$ **to** M **do**
            Project R onto dictionary, pick max atom ϕ_{γ_i};
            Local search around ϕ_{γ_i} using δE as stepsize;
            Move ϕ_{γ_i} towards a better atom;
            Compute $\alpha_{\gamma_i} = \langle R, \phi_{\gamma_i} \rangle$;
            $R = R - \alpha_{\gamma_i} \phi_{\gamma_i}$;
        end
    end
end

Algorithm 2: Parametric Matching Pursuit

Chapter 4

Sparse Encoding of Human Walking

This chapter demonstrates an application of the theoretical framework described in the previous section. We provide an exposition of applying the efficient coding techniques from the previous chapters to muscle length changes captured from human subjects while performing various movements especially walking. We first take a tour of the various tools and techniques employed to obtain the human walking data. Next we apply the efficient coding methods to obtain a sparse code of human walking. Finally, we look at various analyses of the obtained code.

4.1 Methodology

4.1.1 Optical Motion Capture System

In optical motion capture systems, a number of markers are placed on the object being tracked. Optical cameras are then used to track the individual markers on the object. The captured visual information is then processed by the motion capture system and used to triangulate the 3D position of each individual marker. Optical systems can be grouped into two categories: i) Passive, and ii) Active. In passive optical systems such as those produced by Vicon [vic], reflective markers are placed on the object being tracked and strobe lights are then used to illuminate the markers so that they can be tracked by the camera. The main advantage of passive systems over active

(a) Human motion captured using PhaseSpace capture system. Picture represents a subset of all the markers used, see Table **??** for the complete set.

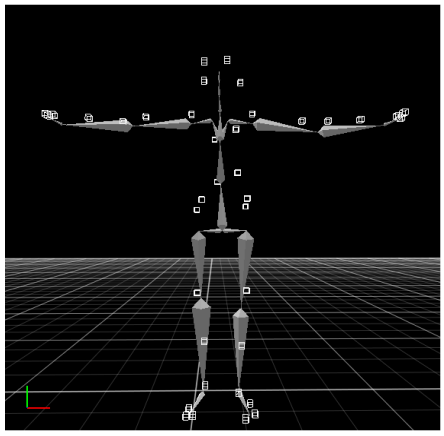

(b) Using Recap2 to generate a full-body skeleton based on a set of training data. This allows to clean up data by constraining markers to bones.

Figure 4.1: Motion capture using Phasespace tools. Active LEDs were used to capture human motion and filtered using custom software.

systems is that the markers placed on the object being tracked does not contain any electronic equipment, thus allowing for more flexibility in certain situations. In active optical systems, the markers contain embedded emitters that allow discrimination between different markers. The main advantage of active systems over passive systems is that each marker can be uniquely identified. This allows for faster resolution of marker overlaps as well as reduce the processing time required to track and distinguish individual markers. As a result, active systems can perform at higher speeds than passive systems at the expense of increased cost and reduced convenience.

We used Phasespace Impulse motion capture system [pha] to capture a human subject's movements. Active LED markers were placed on predefined

Head	Torso	Upper Extremity (each side)	Lower Extremity (each side)
Head.Front	Chest.Front*	Shoulder.Top	Hip.Front*
Head.Top	Chest.Back*	Shoulder.Lateral	Hip.Back*
Head.Back			
		Elbow.Lateral	Knee.Lateral
		Elbow.Medial	Knee.Medial
		Wrist.Lateral	Ankle.Lateral
		Wrist.Medial	Ankle.Medial
		Palm.Dorsal	Toe
		Thumb	Heel
		Middle Finger	Foot.Lateral

Table 4.1: Marker set used for capturing motion. Marker positions with * indicate that two markers were placed at that location.

body parts of a human subject, and observed by multiple overhead cameras, at 480 frames per second using 16 cameras at a one millimeter level of accuracy. Each camera, equipped with two linear detectors, was calibrated prior to the experiment. The system utilizes data captured from these multiple cameras to triangulate each marker and provide accurate, real time location using the projection of the marker on the camera's image plane.

Furthermore, each active LED modulates at a unique frequency resulting in a unique digital ID, recognized by the cameras, hence ensuring no error in recognition of a marker. Table **??** provides the complete set of markers used to capture the motion.

4.1.2 Musculoskeletal Model

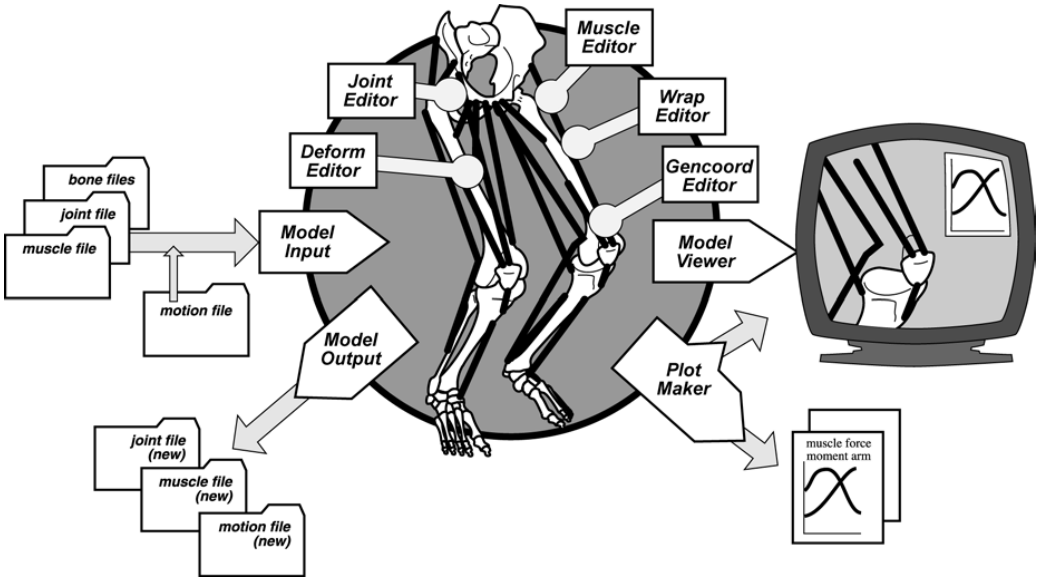

Figure 4.2: Structure of SIMM. Input files describing the bone surfaces (bone files), joint kinematics (joint file), and muscle-tendon parameters (muscle file) are read in to make a musculoskeletal model and information is extracted from the model by making plots, movies, or by exporting edited joint, muscle, and motion files. Figure reproduced from [Delp and Loan, 1995]

We used a musculoskeletal software, SIMM (MusculoGraphics Inc., Chicago, IL) [Delp and Loan, 1995], to translate optical motion capture data to equivalent skeletal angles and muscle lengths.

SIMM (Software for Interactive Musculoskeletal Modeling) is a tool kit that facilitates the modeling, animation, and analysis of three-dimensional musculoskeletal systems. The musculoskeletal model consists of representations of bones, muscles, ligaments, and other structures. and provides various tools (as summarized in Figure 4.2) with editing and analysis functions.

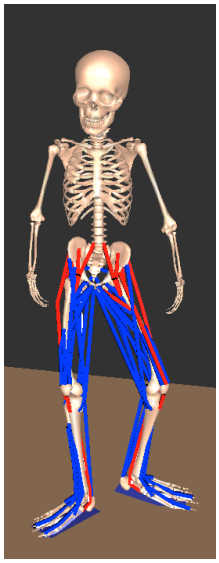

(a) Musculoskeletal model of the human body with muscles for lower extremities.

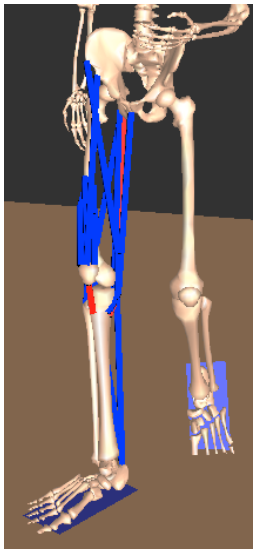

(b) Muscles involved in just the right knee flexion/extension.

Figure 4.3: Detailed musculoskeletal model using SIMM environment. Muscles on the right knee and hips are studied in our simulations

Figure 4.3 shows a SIMM model with forty-four muscles for each limb of the lower body. The parameters used for the lower limb muscle model representing a normal, adult male were created by Delp [1990] based on a model developed at the VA Rehabilitation R&D Center in Palo Alto, California.

We were specifically interested in understanding the principles for generating human-like three-dimensional motions for everyday tasks. Movements that fall in this category are smooth, repetitive motions like cycling, walking, jumping, and running.

To this end, we studied the length change properties of thirty muscles of the right limb that are involved in hip and knee joint movements. The

Gluteal	Anterior thigh	Medial thigh	Posterior thigh
Gluteus maximus	Sartorius	Gracilis	Bicep femoris
Gluteus medius	Iliacus	Adductor longus	Semitendinosus
Gluteus minimus	Psoas	Adductor brevis	Semimembranosus
Piriformis	Pectineus	Adductor magnus	
Gemellus	Quadraceps femoris Rectus femoris Tensor fasciae latae Vastus lateralis, medialis, intermedius		

Table 4.2: Muscles spanning the hip and knee used in our simulations.

musculoskeletal model was scaled and calibrated for the subject using a predetermined pose. Further each joint was represented by two markers (medial and lateral) placed carefully across the joint, such that the joint origin coincided with the midpoint of the segment joining the two markers. This allowed accurate computation of the joint position as the average of the two marker positions and minimized any possible error introduced by assumptions made by SIMM about the position of the marker with respect to the joint.

4.1.3 Other equipment

Horizon Fitness T91 treadmill (Figure 4.4a) was used for walking and running, with speeds between 1 mph to 4 mph, and inclines between 0.5 degrees to 6 degrees. The Oncourt-Offcourt Stroke Trainer (Figure 4.4b) was utilized

(a) Horizon T91 treadmill for walking and running motion capture

(b) Stroke Trainer tool for repeated swings

Figure 4.4: Accessory equipments used for the motion captures.

to obtain a stationary target for repeatable tennis strokes. Height for the stationary ball was between 100 cm and 120 cm off the ground.

4.2 Encoding and analysis of human movements

This section reports a number of results using the PMP model. We show the performances of the PMP model in representing walking movements for multiple subjects at various speeds and incline surfaces.

4.2.1 Encoding of lower limb muscles

Eight healthy adults from the graduate students in the Computer Science department of the University of Texas at Austin volunteered to be

captured using the motion capture system. Each participant was instructed to walk for five minutes, run for one minute, and jump for one minute. Their muscle length changes were computed from their motion capture as described in Section 4.1.2.

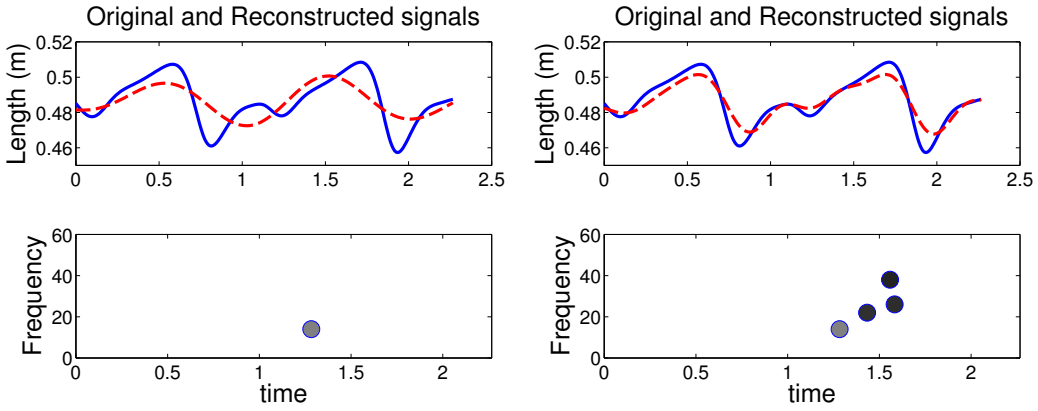

(a) Reconstruction with a single basis functions

(b) Reconstruction with 4 coefficients

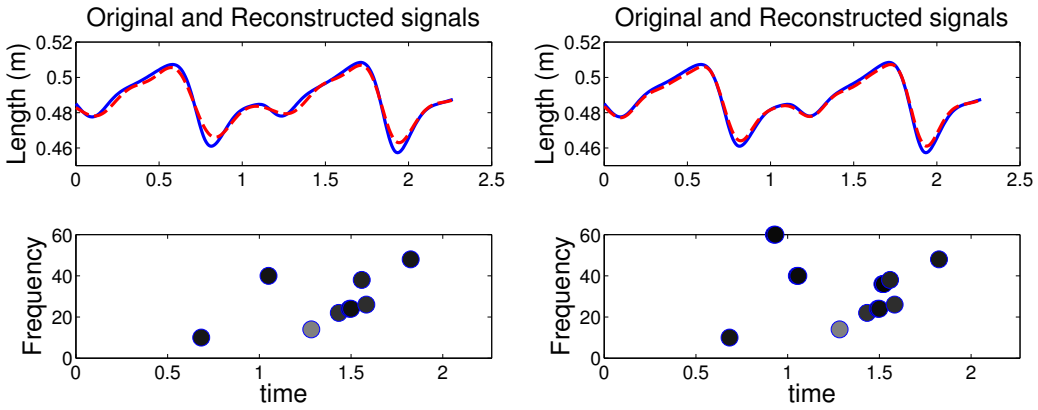

(c) Reconstruction with 10 coefficients

(d) Reconstruction with 20 coefficients

Figure 4.5: Sparse coding of the Gracilis muscle for two steps of walking. Each circle represents a basis function with two dimensions (time and frequency) of the basis function represented in the figure.

Figure 4.5 illustrates the sparse code result and its efficiency in

representing the Gracilis muscle using a fixed set of basis functions. Each circle represents the temporal position and center frequency of an underlying function, with the gray value indicating the amplitude of the function. The figure shows that only a small set of atoms (less than 25) is sufficient to produce an accurate reconstruction of the muscle length with more than 300 samples.

Figure 4.6 illustrates the muscle length changes and the accuracy of representing it using our model for some of the hip, knee, and ankle muscles. The figure shows an accurate reconstruction of the muscle length changes with more than 300 time samples using about 20 coefficients. Muscles have a stationary, relaxation length and each muscle produces displacement around that length. As figure 4.6 shows, different muscles work around different relaxation lengths and the advantage of using a multi-scale dictionary is that it enables the use of a single dictionary for all such muscles. The error in the reconstruction of each of the muscles in the figure is minimal.

The algorithm provides an accurate reconstruction of the muscle lengths, but movement in the original skeletal model is represented as joint angles. To visualize the reconstructed muscle changes in the model, and compare it to the original data, the reconstruction had to be converted to generalized joint angle coordinates. Each angle of a joint uniquely determines the lengths of all muscles spanning it, but the reverse is not necessarily true. For a single muscle, given its length, we cannot necessarily determine a unique angle for the joints it spans. This is true for most of the biarticular muscles (muscles that cross two joints). For an arbitrary set of biarticular muscle lengths, there could be a number of joint angle solutions (or possibly none, for the case where the muscle lengths are erroneous). Hence, an optimization criterium that generates the "best" joint angle for a given set of muscle lengths

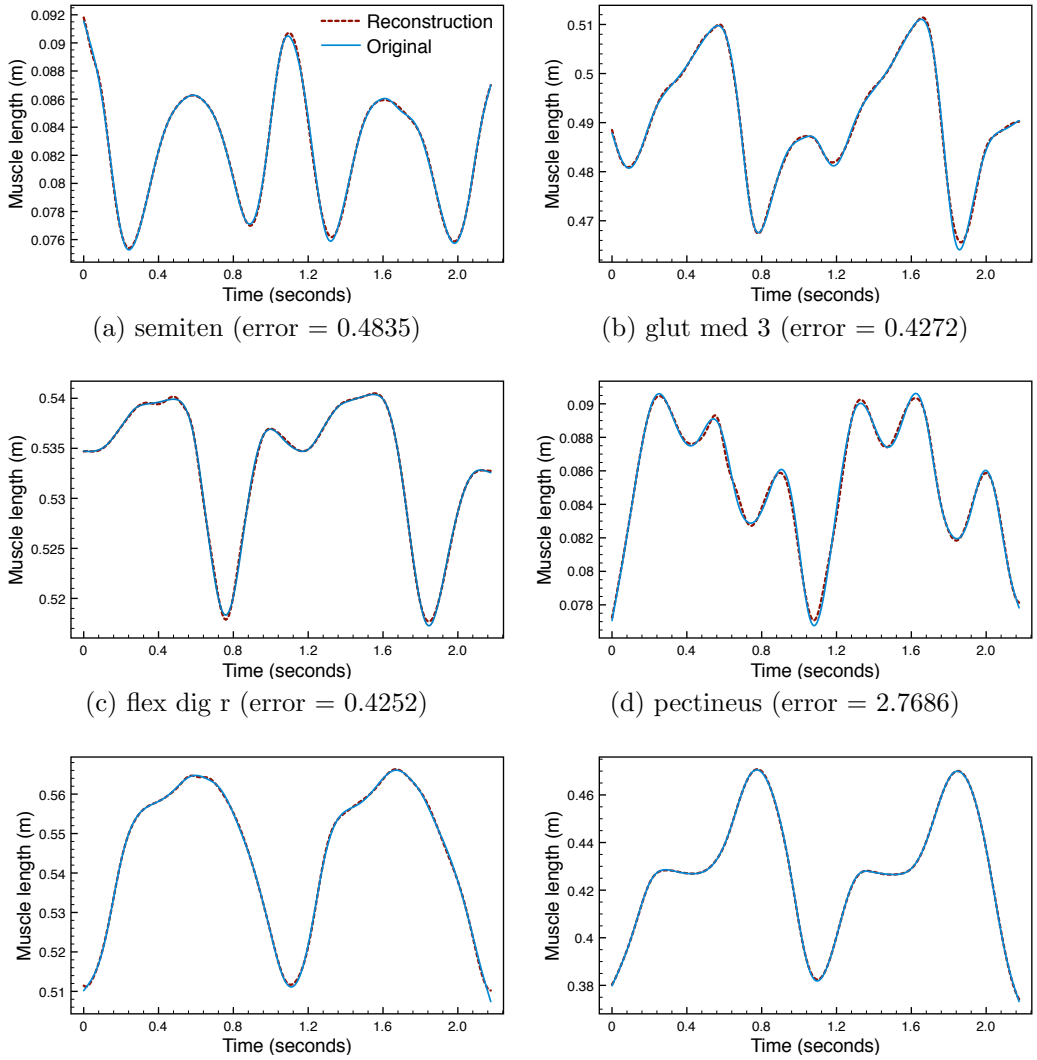

(a) semiten (error = 0.4835)

(b) glut med 3 (error = 0.4272)

(c) flex dig r (error = 0.4252)

(d) pectineus (error = 2.7686)

(e) bi fem sh (error = 0.4649)

(f) gas lat r (error = 1.0635)

Figure 4.6: Reconstruction of the length of various lower body muscles of the right limb during two steps of walking. Note that the scale in each axis is different.

is necessary. The problem is similar to the Inverse Kinematics (IK) problem for controlling the movement of a rigid multi-body. In the case of IK, settings

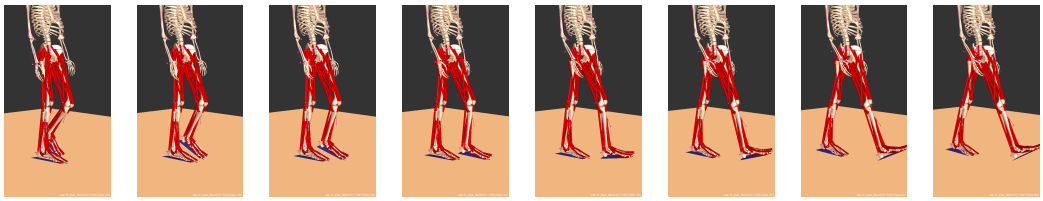

Figure 4.7: Human walking using reconstructed muscle data obtained by Parametric Matching Pursuit with a multi-scale Gabor dictionary.

for the joint angles are computed so that the resulting configuration of the multi-body places each end effector at its target position. The process is simplified for monoarticular muscles (involved in only one joint), as they form a one-to-one relationship with the angle of the joint they span. Examples of monoarticular muscle include the three vastus heads of the quadriceps femoris (knee extension) and the short head of biceps femoris (knee flexion). These muscles were used to uniquely determine the knee angle for any set of muscle lengths.

Figure 4.8 displays the muscle-angle relationship for the knee. Many of the hip muscles, however, are responsible for more than one type of movement in the hip, as different areas of the muscle act on tendons in different ways. The iliopsoas (psoas major assisted by the iliacus muscle), is the primary hip flexor, and the gluteus maximus handles the extension. Medial hip rotations are performed by glutaei medius and minimus, and lateral rotations by the lateral group, especially the piriformis and gemellus muscle. Hip adduction is handled primarily by the adductor group of muscles and hip abduction by the gluteus medius muscles [Tortora., 2005].

Figure 4.9 shows the joint angle trajectories found using a brute force search over the primary muscles for the corresponding angles. The figure

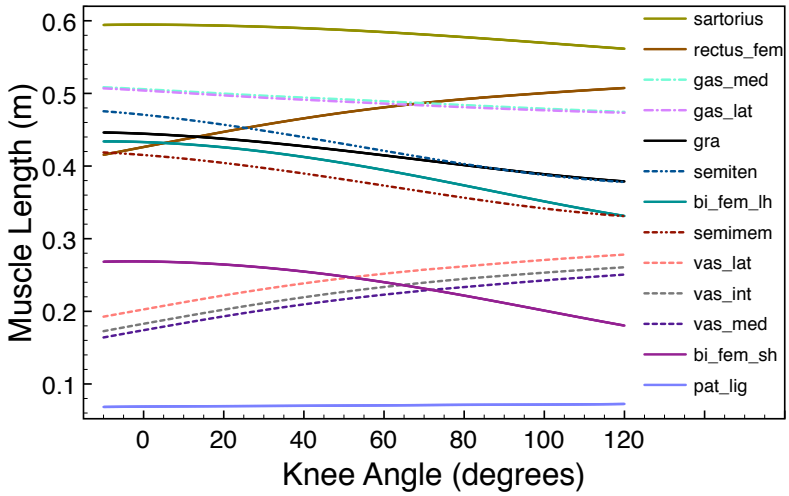

Figure 4.8: Muscles spanning the knee plotted for varying values of the knee angle. Even though the figure implies an injective relationship between the muscles and knee angle, only the monoarticular muscles (patellar ligament; vastus heads - medialis, lateralis, intermedius, and short head of bicep femoris) can be used to compute the knee angle from muscle length.

includes knee flexion (4.9a) and the three angles for the hip (flexion 4.9b, adduction 4.9c, and rotation 4.9d). The knee angle is computed by searching over vastus head muscles and the bicep femoris (short head), with minimal error due to the monoarticular nature of the muscles. The smooth nature of the Gabor functions also eliminated the noise elements in the original joint angle trajectory. The reconstruction for the hip angles, however, was not exact. Muscles used to calculate hip joint angles are shown below.

- Hip flexion: Iliacus, psoas, gluteus maximus,
- Hip rotation: Piriformis, gemellus, gluteus medialis,
- Hip adduction: Adductor brevis, gluteus minimus.

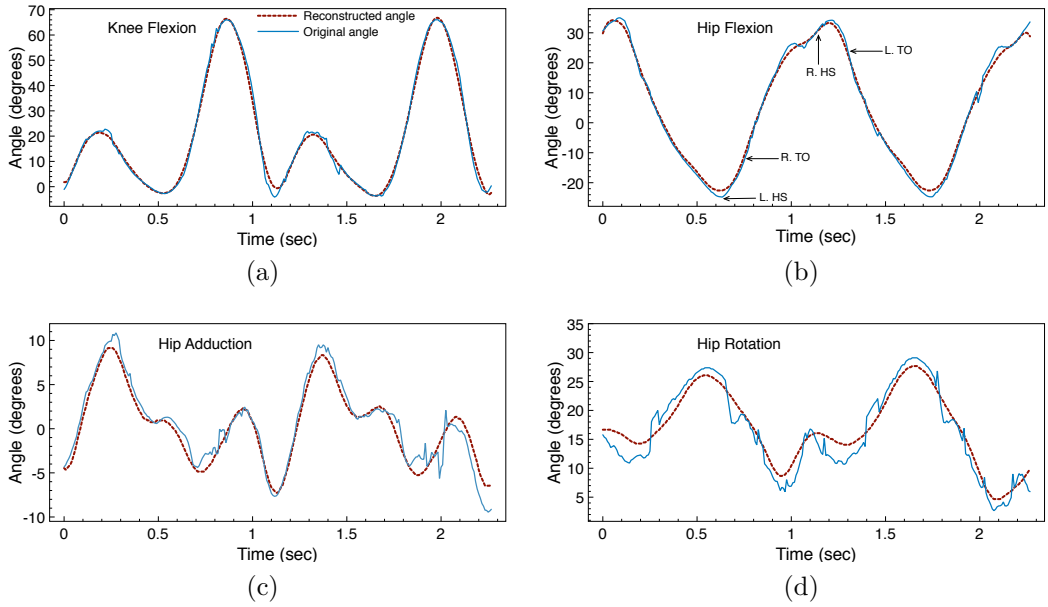

Figure 4.9: Joint angles reconstructed from the sparse-code representation of the muscle lengths. High frequency noise elements exist in the few frames because of marker dropouts in the motion capture. The noise is rightly ignored in the reconstruction, due to the smooth nature of the Gabor atoms. Figure 4.9b shows the heel-strikes (HS) and toe-offs (TO) of both feet for one of the two steps.

The hip muscles did not map as well as the knee, primarily due to the overlap of various muscles' involvement in different joint angles. The reconstruction still retained the general nature of the hip movements, and when viewed in the original model, the movement pattern thus obtained (example in Figure 4.7) was similar to the original captured movement.

4.2.2 Optimizing basis functions

Two parameters were manually set before the learning algorithm computed the best possible dictionary: the number of atoms in the dictionary

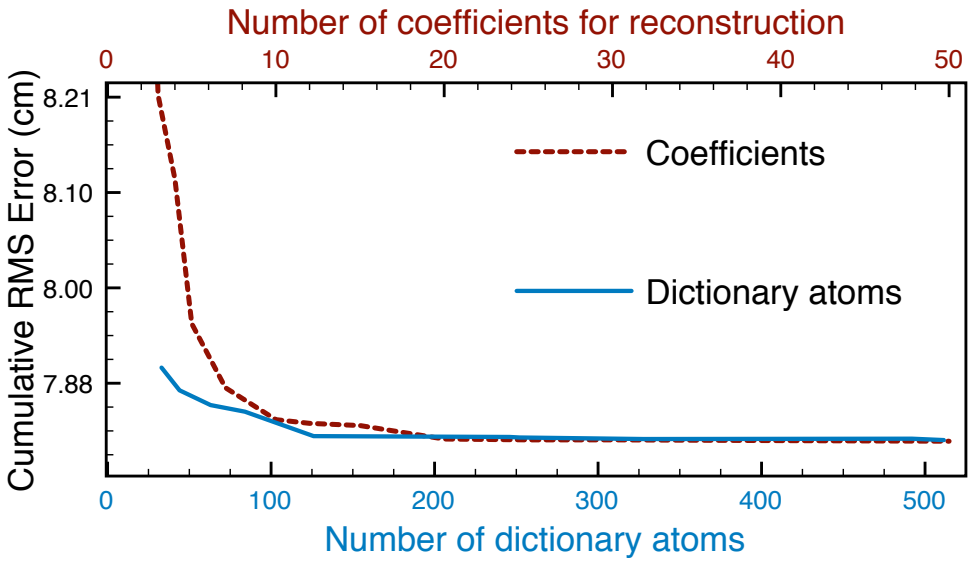

Figure 4.10: The effect of changing the number of coefficients for reconstruction and varying the number of dictionary atoms on the accuracy of reconstruction. To study the size of the dictionary, number of coefficients were set at 20, and for the coefficients case, dictionary size was set to less than 200 atoms.

and the number of basis elements (coefficients) to combine for each muscle. Figure 4.10 illustrates the effect of change in these parameters on the root mean square error (RMS) averaged for all muscles in all the movements. For either parameters, we can see that the error is high for low number of resources, but quickly reached a baseline. For the final reconstruction results shown here, we used a dictionary size of 492 elements and combined 20 basis elements to reproduce each muscle.

4.2.3 Measuring Coding Efficiency

The previous section shows that sparse coding provides good representation of motor functions, but it is not yet demonstrated that this is an efficient representation. Such an evaluation requires an objective measure of 'efficiency'. We employ Shannon's rate-distortion measure used by Smith [2006] to compare various encoding algorithms for auditory signals. The idea is to vary the rate of a code (typically in terms of coefficients/second) while measuring the distortion of the signal, such as mean squared error.

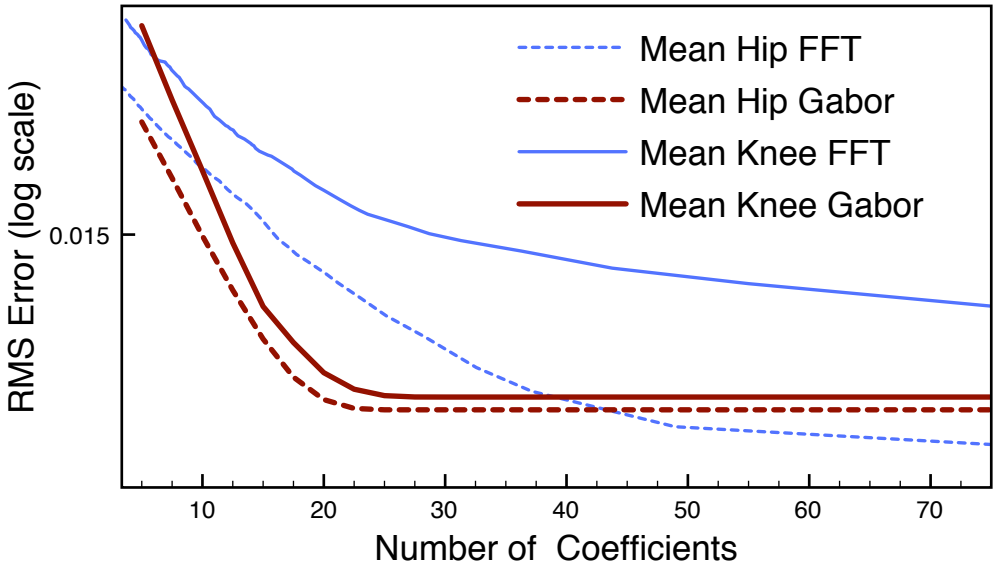

Figure 4.11: Comparing fidelity of reconstruction by Fourier transform and PMP with Gabor functions

We compared the coding efficiency of a Gabor dictionary with the fidelity of coding the same signal using a windowed Fourier transform of the signal. The overcompleteness of the dictionary ensured that for low number of coefficients, the Gabor representation provides a high fidelity signal.

Figure 4.11 shows the performance comparison between the two representation forms. For relatively small number of coefficients (less than thirty-five), the Gabor representation produced a minimal-error reconstruction. The Fourier representation, in some cases, required more than twice the number of bandwidth to give the same fidelity. The shortcoming in the overcomplete representation is that the reconstruction does not get to zero error, primarily due to the dictionary missing higher frequency elements. Excluding the high frequency elements does, however, avoid the possibility of treating external noise as part of the signal.

4.3 Analyzing coefficients

The previous section showed how we can decompose a movement signal to set of coefficients of an optimized dictionary. It would be interesting to measure the fidelity of these coefficients for repeatable actions of such movements. Different affordances lead to subtle changes in movements, and it would be beneficial to detect these hard-to-detect changes using coefficients.

4.3.1 Walking at different speeds

Four healthy young adults (all male) from the graduate student population of the University of Texas at Austin volunteered to be participants for this experiment. All participants provided informed consent before testing began. Participants were then given an opportunity to become familiar with treadmill walking at the experimental speed for a period of 5 min. During this time participants were given instructions on how to begin walking on the moving treadmill. We captured walking at four speeds (2.0, 2.5, 3.0, and 3.5 miles per hour) for each subject.

Thirty muscles were analyzed and encoded using PMP. In total, 200 dictionary atoms were used for the reconstruction, with each encoding instance computed using 15 coefficients. To analyze the differences in encoding results between different subject-speed combinations, we concatenated the coefficients for all muscles in a single vector, resulting in a 6000-element vector. We applied Principal Components Analysis (PCA [Joliffe, 1961]) on this high-dimensional vector to extract the dimensions that project to the highest variability. In the MATLAB Statistics Toolbox, the functions *princomp* was used to compute the principal components, while the function *pcares* was used for the residuals.

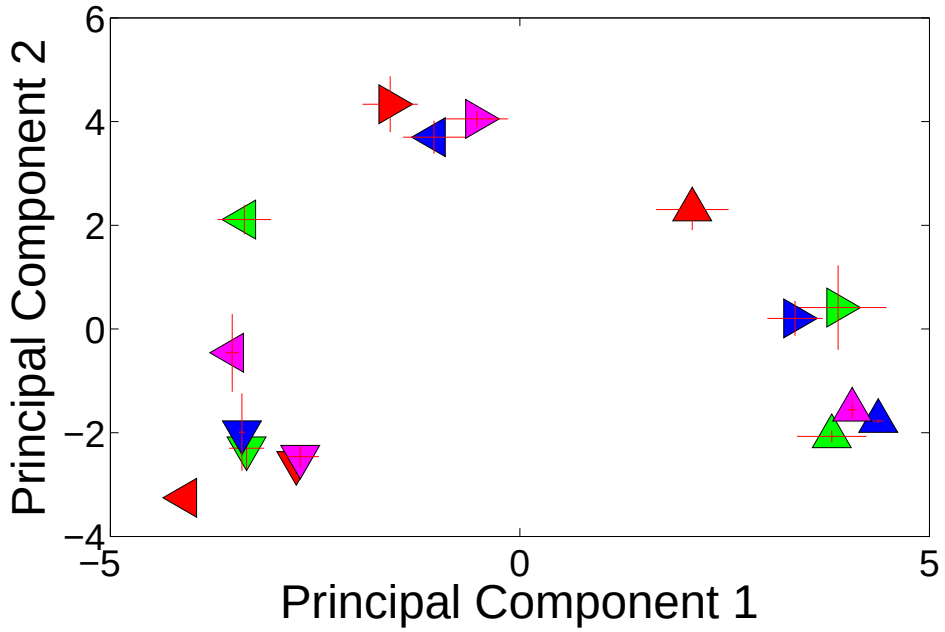

Figure 4.12: Principal component projection of the encoding for walking at multiple speeds. ▼ = 2.0mph, ◀= 2.5mph, ▶= 3.0mph, ▲ = 3.5mph. Each color represents data from 1 subject.

Figure 4.12 shows the projection of the coefficient vector over the first two principal components. Each subject is plotted with a specific color and

the speeds are plotted as described in the figure. We can see a clear separation between the coefficients for walking at 2.0 mph compared to walking at 3.5 mph. There is a progression of the coefficients from the 2.0 mph case (▼) to 3.5 mph case (▲). There is a wider spread for the intermediate speeds, but it is important to note that for any one subject the separation between speeds is apparent. We can conclude from this result that the walking movements at different speeds are characteristically different. The difference in the coefficients are primarily in the frequency of the basis functions (not shown in figure), with higher speeds resulting in higher frequency bases. The movements across subjects, however, are similar for each speed set and is emphasized at the extreme speeds (▼ and ▲).

4.3.2 Walking on incline surfaces

During walking, the pelvis and trunk move in the three anatomical planes and three-dimensional analyses reveal very complex patterns of motions between pelvis and trunk. Similar to section 4.3.1, four subjects took part in the experiment. The subjects walked on a treadmill at four different grades (1%, 3%, 7%, and 10%) without any assistance. Here each percentage grade represents 0.58 degrees in angle. Several practice trials were used to familiarize the subjects with treadmill walking and to determine the subjects comfortable walking speed.

Same as section 4.3.1, a PCA analysis was performed on the basis encoding of the movements. In contrast to the speed encoding, walking at different inclines was appreciably prototypical.

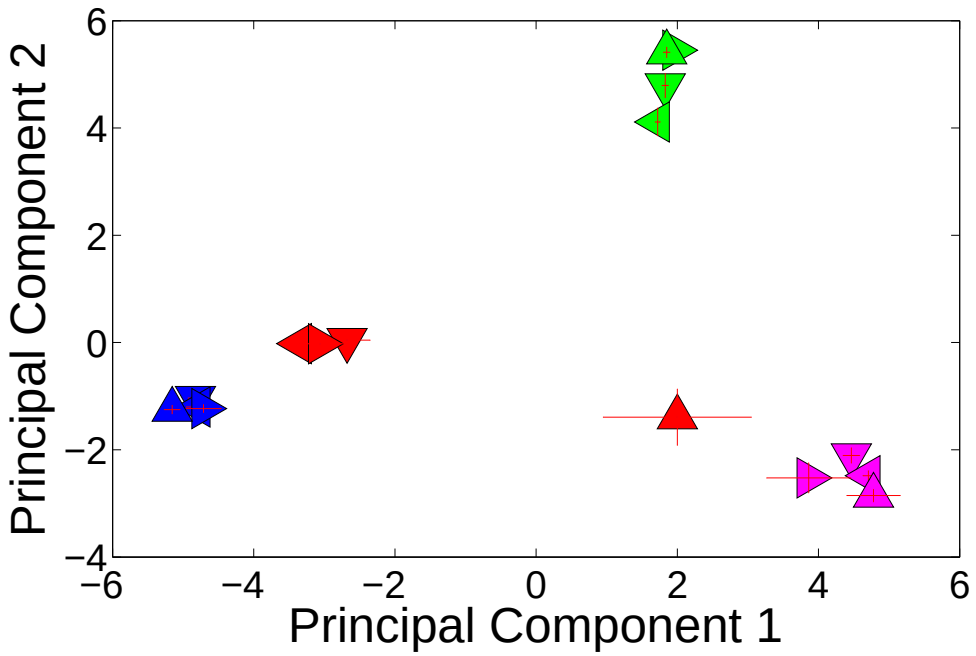

Figure 4.13: Principal component projection of the encoding for walking at multiple inclines. ▼ = 1%(0.58°), ◀= 3%(1.74°), ▶= 7%(4.06°), ▲ = 10%(5.8°). Each color represents data from 1 subject.

4.3.3 Adaptation to unilateral change in lower limb dynamics

In order for the central nervous system (CNS) to effectively control the movement of the lower limbs during locomotion it must have some implicit knowledge of the mechanical properties of these body segments. This knowledge is necessary to achieve the desired lower limb kinematics during locomotion by recruiting the appropriate muscles at the appropriate magnitudes. Noble and Prentice [2006] presented evidence that humans show an adaption in their limb movement during walking when a weight is added unilaterally in a lower limb. Similarly, an adaption is seen when the weights are removed after recalibration of the movements with weights. We replicated the

results from [Noble and Prentice, 2006] using our basis function representation. The objectives of this experiment were bifold: reflect the precision of our sparse-code representation and present evidence for adaptability in human movements for such mechanical limb property changes.

Experiment

We replicated the same experimental procedure as employed by Noble and Prentice [2006]. Four healthy young adults (all male) from the graduate student population of the University of Texas at Austin volunteered to be participants for this experiment. All participants provided informed consent before testing began. Participants were then given an opportunity to become familiar with treadmill walking at the experimental speed for a period of 5 min. During this time participants were given instructions on how to begin walking on the moving treadmill. Participants then walked on a motor driven treadmill with a belt speed of 1.56 m/s (3.5 mph). This particular speed was selected to be slightly faster than the natural walking speed of all participants in order to provide a greater challenge to the locomotor control system.

The participants performed three 5 min walking trials on the treadmill. During the first trial the participants walked on the treadmill for 5 min with no additional mass placed around the leg segments (PRE condition). Following the initial 5 min walking trial, a 2 kg mass was attached around the center of mass of the leg segment of the left lower limb. The mass was placed over the lower half of the muscle mass of the calf. The mass was secured to a non-slip velcro strap, and an elastic bandage around the outside of the mass. Care was taken to ensure that blood flow was not occluded by the attachment of the mass. The participants then walked on the treadmill for a period of 5 min

with the 2 kg mass attached their left leg (WEIGHT condition). The mass was then removed and the participants were immediately required to perform another 5 min trial of treadmill walking (POST condition). Kinematic data were collected for the entire 15 minute duration of the walking trials.

Results

For our pilot study, we conducted the above experiment with two subjects walking without and with the weight attached to the calf. We encoded the muscle lengths using PMP and applied PCA on the concatenation of all basis coefficients. Each stride was treated as a single data point for the PCA analysis. Figure 4.14 illustrates the projection of the data to the top two principal components. The colored circles represent the PRE condition while the colored plus symbols represent the strides in the WEIGHT condition. The basis functions were modeled with the PRE condition data, leading to higher variability in representing the WEIGHT condition data.

The above observation leads us to two conclusions. First, the sparseness and robustness of the learning algorithm is evidenced from the low variability in representing the PRE strides and the high variability in WEIGHT stride coefficients. Even though the WEIGHT condition strides were qualitatively walking movements, the variability in the strides becomes apparent through the coefficients. Second, the stride-to-stride variability in the two subjects indicate that the sudden change in the inertial properties of the leg led to a difficulty in walking. This increases our confidence in the involvement of the motor primitives for motor control. The motor system planned the walking movement with an "internal model" of the leg dynamics. Adding the weights leads to a discrepancy between the model and reality, resulting in irregular

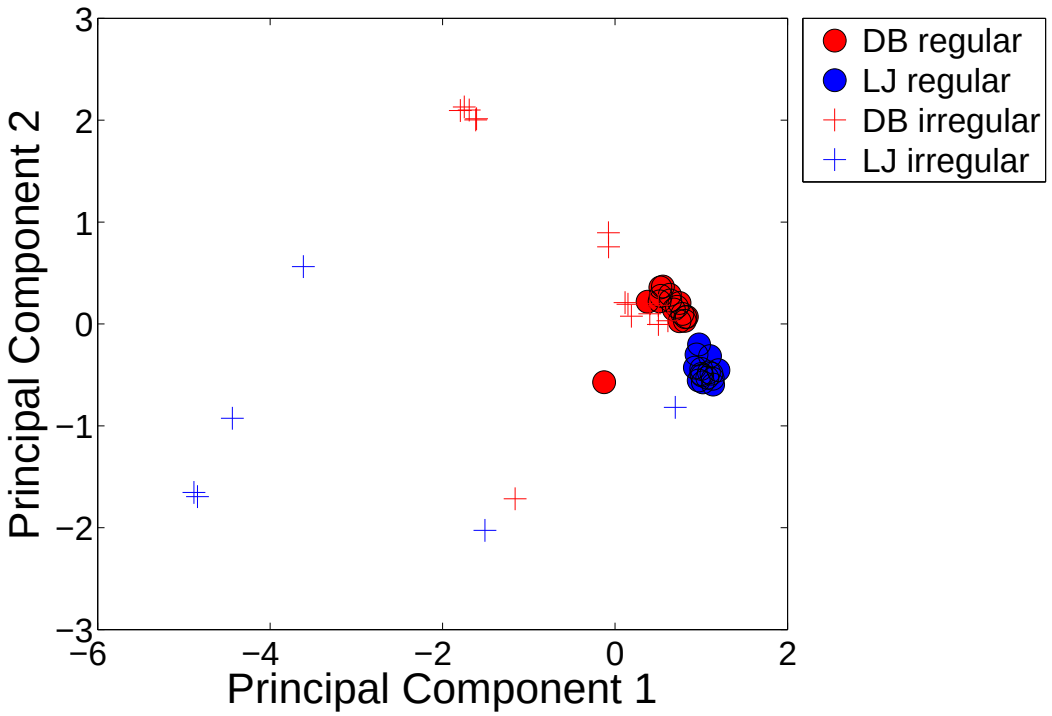

Figure 4.14: Basis function coefficients can be a reliable indication of the movement pattern. The first two principal components of coded stride data taken from two subjects under different conditions using the coefficients for for all muscles in a concatenated vector. Irregular data represents the movements obtained by adding a 2 kg mass on calf and are represented by +, while the regular data is simple walking, represented by •. The two colors represent the two subjects. A clear distinction between the normal and irregular samples is observed. The hypothesis is that PCA should reveal different clusters for planned and unplanned movements situations, owing to the basis functions modeled with the regular data.

walking patterns.

Figure 4.15 gives the same projection as figure 4.14 for all four subjects. Here we average over all projections of coefficients for individual subjects. The bars on each data point indicate 1 standard deviation. Once again we can see

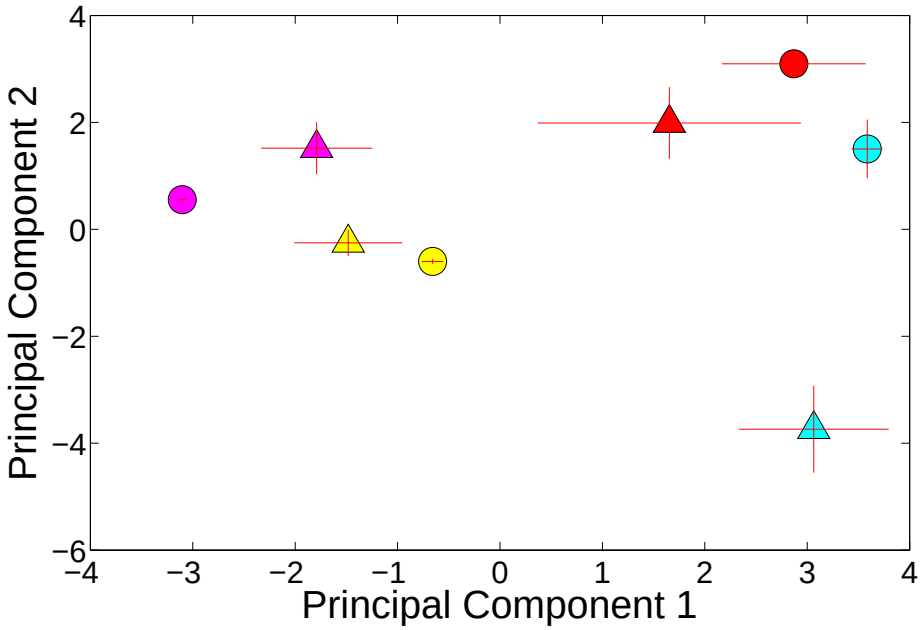

Figure 4.15: PCA projection of the combined coefficient vector comparing movement variability in walking. Each circle represents the projection of the coefficient averaged over all walking strides of a single subject. Each triangle represents the average projection while walking with a 2 kg load on the leg. Each individual subject is plotted with a different color.

that on training the dictionary for normal walking, we get higher precision when representing the normal walking test data over the walking with weights data. This confirms that the basis function encoding are indicative of human movements.

4.4 Discussion

In the previous chapter we discussed a theoretically-motivated model for muscle length changes where the computational goal is to form an efficient, representation of the time-varying signal. Movements are represented by

decomposing them into a minimal number of Gabor functions, each with an associated time, frequency, scale, and amplitude. We have shown that this yields efficient representations of transient signals. We have also shown that over a large range of coefficients, this representation is more efficient than Fourier representations.

Another view of these results is that we have shown a method for achieving significantly greater coding efficiency using a parametric approach to an overcomplete basis. A motivating goal for overcomplete representations is to use a rich dictionary of signal descriptors to find compact signal representations. The number of basis functions in such a case, can be arbitrary numerous in frequency and time. The advantage offered by the approach here is that it is not necessary for the code to describe each implicit coefficient (i.e. at every sample position). Instead, a parametric set can represent the specific time and frequency for necessary basis functions learned from the data.

The basis functions learned from the captured data provide a succinct description of the movements. We presented evidence on the usefulness of this description by distinguishing walking at different speeds. The basis coefficients provide a tool to understand and label different movements and classifying such movements is a simple matter of partitioning easily-separable coefficients. The high variability in encoding different speeds indicates that there is voluntary change in movement structure while increasing speed. On contrary, relatively invariable coefficients for various inclines suggest that the basis walking patterns remain same for different inclines. There is, however, a change in the force output, necessary to oppose the higher gravitational pull. We believe that the control signal sent to the muscle for different inclines uses the same coefficient, but there is a higher muscle output due to the difference

in the expected state and the actual state achieved. For example, if the foot is expected to be on a flat ground, but due to the incline, there is a disparity, then additional forces are applied to eliminate the disparity. The force applied by the muscle is proportional to this difference. This theory is further explored in Appendix B.

Chapter 5

Extending Sparse Encoding

The previous chapter showed an efficient way to represent human movements as a superposition of non-linear functions. The basis decomposition provides an low-bandwidth solution to produce accurate reconstructions of muscle signals. In this chapter, we extend the usefulness of the basis functions by introducing the notion of 'synergies'. Further, we gloss over a framework that allows us to learn new trajectories from pre-learned coefficients of related, but different movements. We performed a pilot-study to explore this framework and provide an exploratory analysis of the results.

5.1 Synergistic Movements

As discussed earlier, the central nervous system (CNS) has more degrees of freedom than necessary, requiring it to resolve among a theoretically infinite number of solutions, resulting in the famous problem of redundancy (the Bernstein problem, [Turvey, 1990; Latash, 1993]). Consider, for example, the problem of touching the tip of your nose. The location of your nose has three degrees of freedom (its x, y, and z position in Cartesian coordinates), but the joints of your arm have seven degrees of freedom (the shoulder has three degrees of freedom, and the elbow and wrist each have two). Consequently, there are many different settings of your arms joint positions that all allow you to touch your nose. Which setting should you use?

A lot of research has been motivated by Bernstein's suggestion that the CNS unites elements into groups such that each group is controlled by a single variable. Bernstein called such groups, synergies. The presence of such synergies decreases the number of variables the controller needs to manipulate and (partly) solves the problem of redundancy. In a sense, the physiological organization of muscle fibers into motor units may be viewed as a low-level synergy, which allows the controller not to bother about individual muscle fibers but to deal with a fewer number of motor units.

So, according to Bernstein, the CNS organizes elements (joints of a limb, muscles acting at a joint, fingers of the hand, etc.) into synergies in a task-specific, flexible way. Ultimately the problem of motor redundancy is solved and a single optimal solution emerges. Related to this interpretation, others have suggested that muscle synergies provide a way for the CNS to bootstrap complex problems of optimal control; by identifying a task relevant subspace of control variables, the potentially difficult problems of optimization would be minimized.

Dating at least back to the work of Sherrington [1910], several researchers have proposed that the CNS produces movement by combining small groups of muscles [see Tresch and Jarc, 2009, for more details]. We employ this well-researched idea of synergies to extend our sparse encoding technique, by combining the code for multiple muscles across a group to show and increased reduction in the dimensionality for representing movements. We first look at the synergies existing in the data by analyzing correlation between muscle activations. Encoding patterns can be shared between correlated muscles during the reconstruction to reduce dimensionality of the movement code.

Synergistic coding is attractive both as a more compact code, but also as a model of the underlying organization of the spinal cord [Kiehn et al., 2010]. Muscle synergies have been characterized since Bizzis pioneering work showed that microstimulation in the frog spinal cord activated several different muscle groups [Giszter et al., 1993]. This organization may be anticipated by the cortex as can be seen in microstimulation in monkey cortex leading to patterns of inter-muscle coordinated movements [Graziano and Aflalo, 2007].

5.1.1 Correlations in lower limb muscle trajectories

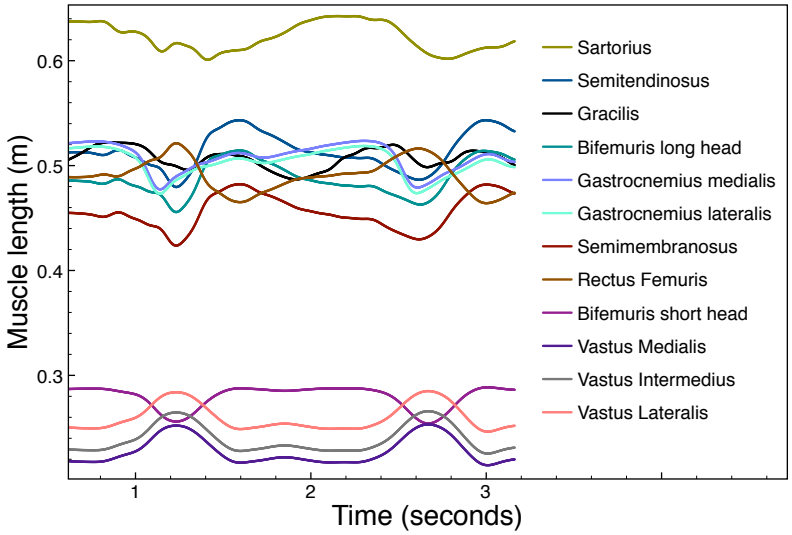

Figure 5.1: Correlations in muscle trajectories. Some muscles of the knee undergo a similar transformation, suggesting a synergy between them. For the knee, the 3 vastus head muscles form a synergy with the bifemuris short head, and the semitendinosus, Bifemuris long head, and semimembranosus form another synergy.

Figure 5.1 illustrates the muscle trajectories for all muscles involved in flexion/extension of the knee while walking. We can see the muscle length changes for two steps taken by the human subject. The figure shows that there

exists a correlation between some of the muscle output. We can group such related muscles as a synergy. Similar correlations in muscle output also exist in the muscles that control the hip.

Figures 5.2 and 5.3 illustrate the correlation between different muscles while walking at a normal speed. As visible in the figure, we have two synergies in the muscles spanning the knee and five synergies in the hip muscles. The synergies are summarized as follows:

Knee synergies

1. Vastus Medialis, Vastus Intermedius, Vastus Lateralis, Bifemuris Short Head
2. Semitendinosus, Bifemuris long head, and Semimembranosus

Hip Synergies

1. Set of 3 Gluteus Maximus muscles
2. Set of 3 Gluteus Minimus muscles
3. Set of 2 Gluteus Medialis muscles
4. Set of 3 Adductor Longus muscles
5. Adductor Longus, Illiacus, Pectineus, Psoas, Tensor fasciae latae

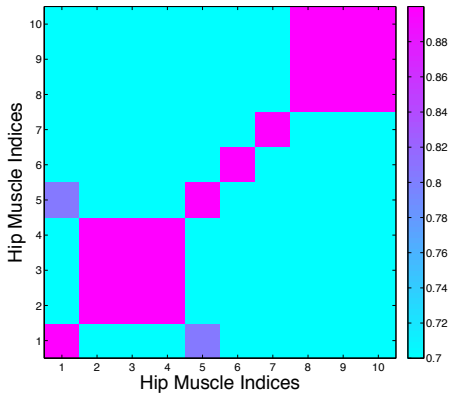

(a) Subject DB

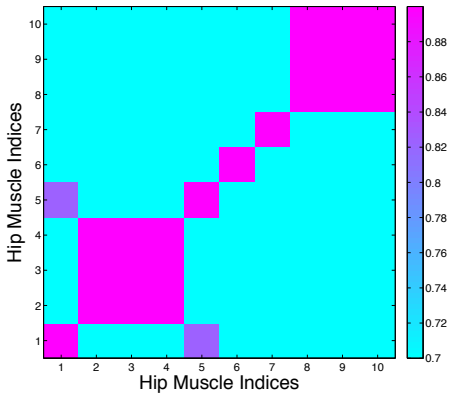

(b) Subject DK

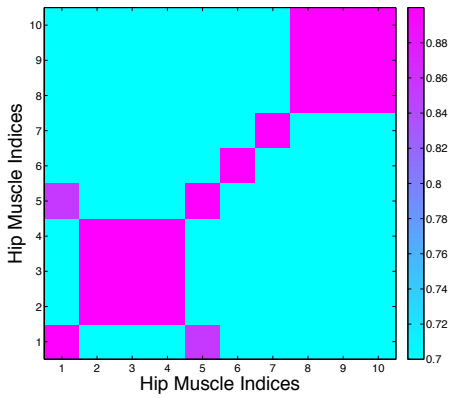

(c) Subject LF

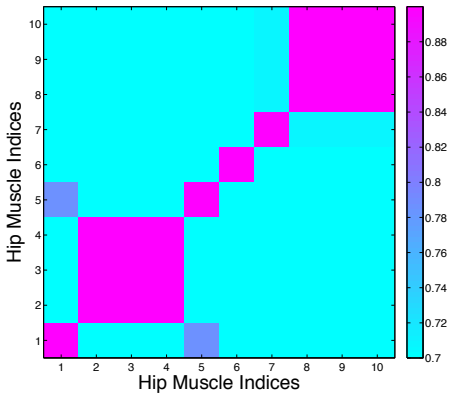

(d) Subject WR

Figure 5.2: Average correlation in the responses of the muscles spanning the knee. The heat map is thresholded to only show correlation coefficients between 0.7 and 0.9. The pink region indicates a correlation exists with a p-value=0.1. The correlation responses are consistent across all subjects and suggest strong synergies. We can see that there are two sets of muscles that are correlated to each other (the smallest pink block indicates that each muscle is correlated to itself).

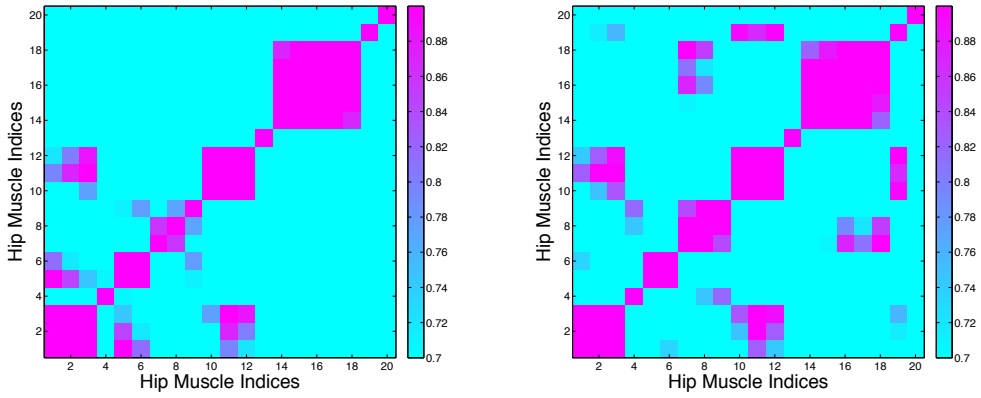

(a) Subject DB

(b) Subject DK

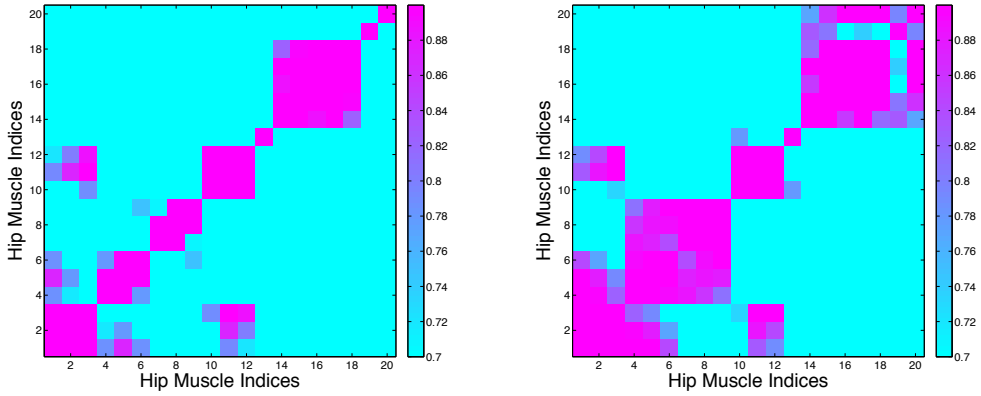

(c) Subject LF

(d) Subject WR

Figure 5.3: Average correlation in the responses of the muscles spanning the hip. The heat map is thresholded to only show correlation coefficients between 0.7 and 0.9. The pink region indicates a correlation exists with a p-value=0.1. The correlation responses are not as consistent as in the case of the knee, but we can still pick, conservatively, five sets of synergies.

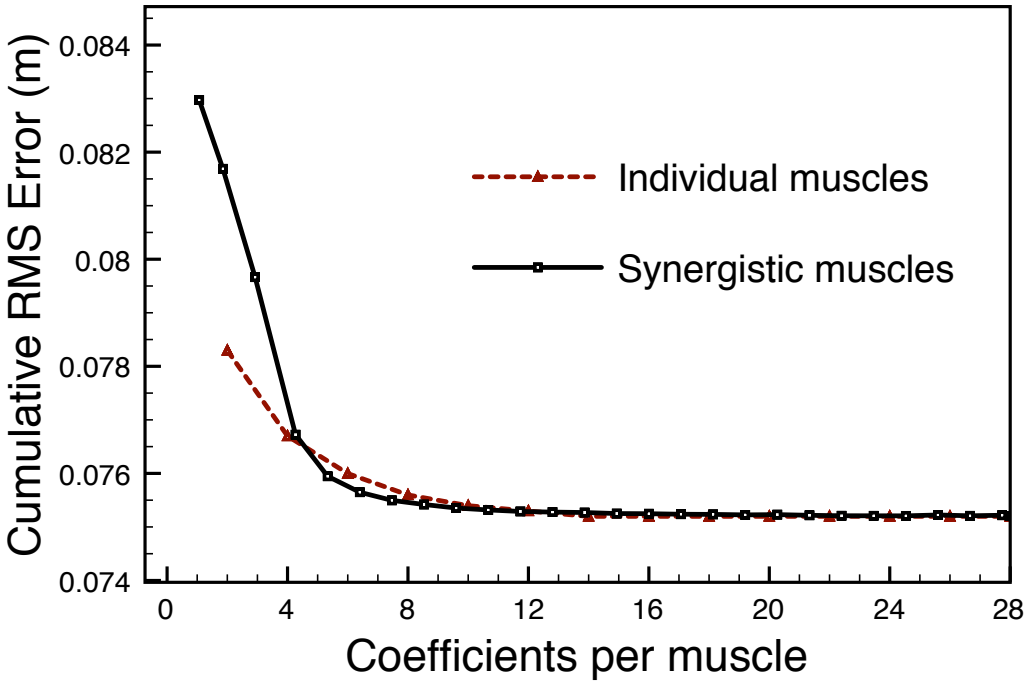

Figure 5.4: Comparison of distortion in encoding individual and synergistic muscles.

In the single-muscle version of the sparse code the coefficient for each basis function, α in Equation 3.1, is a scalar quantity, but this can be extended to multiple muscle codes in a straightforward way by making the coefficient α a vector, with one entry for each muscle component. In other words in synergistic coding, a single basis function can be a part of the length component of different muscles as long as there is a different coefficient value for each muscle. This reduces the process of projection of multiple coefficients to a single group projection. Thus, for five-muscle synergy, instead of five different update signals, we only have a single update for the dictionary. Similarly during reconstruction, only a single projection is required, reducing the reconstruction

time.

Figure 5.4 shows the distortion measure comparison (error per coefficient) between encoding each muscle individually compared to encoding a complete synergy. The error is computed as a root-mean-square averaged over all muscles, all strides, and all subjects. As seen in chapter 4, the total error drops exponentially as we increase the number of coefficients. The efficiency in encoding muscles using synergy is lower for low number of coefficients. This difference, however, is minimized by adding more coefficients.

5.2 Path integrated Jacobian

Applying Parametric Matching Pursuit (PMP) to the muscle data obtained from SIMM, gives a basis function representation of the trajectory made by each muscle. We need a mechanism to correlate this representation with goals existing in the task space. Let's consider specific goals for the end-effectors of the body. If there are k end effectors, let their positions be denoted as $s_1, s_2, \ldots s_k$. Each end effector position s_i is a function of the joint angles that are part of the kinematic chain leading up to the end effector. Each joint angle in turn is a function of the length of various muscles that span that joint. The complete configuration of the robot body is specified by the scalars $\theta_1, \ldots \theta_n$, assuming n joints. $\vec{s} = (s_1, \ldots, s_k)$ is a function of $\vec{\theta} = (\theta_1, \ldots, \theta_n)$ and, further, each θ_j is a function of the muscles spanning the joint represented by $\vec{x_j} = (x_{1j}, \ldots, x_{lj})$.

Thus the end effector position can be obtained from the muscle lengths as,

$$s_i = S_i\left(\Theta\left(X(\vec{\alpha})\right)\right),$$

where,

$$\begin{aligned} S_i &= \text{transformation from angles to end effector,} \\ \Theta &= \text{transformation from muscles to joint angle,} \\ X &= \text{PMP reconstruction of muscle from coefficients } \vec{\alpha}. \end{aligned}$$

We have thus obtained a representative model for end effector trajectories using basis coefficients. A natural next question is how to update these coefficients in the coefficient space to generate new trajectories in the task space, without going through the reconstruction process? The transformation from muscles to angles should be linear and relatively straightforward in well-behaved situations. Unfortunately, this is not true for generating angles for arbitrary end-effectors and generating coefficients for corresponding arbitrary muscle lengths. We can, however, approximate the non-linear transformation from coefficients to end-effectors using a linear Jacobian matrix. The idea would be to use the inverse Jacobian matrix to compute a small change in coefficients that leads to an arbitrary small change in the end-effector.

The kinematic Jacobian matrix J_θ, that describes the transformation from joint angle to end effector, is a function of the $\vec{\theta}$ values and is defined as,

$$J_\theta(\vec{\theta}) = \left[\frac{\partial s_i}{\partial \theta_j}\right]_{ij}$$

Extending the same to muscle lengths, J_α describes the transformation from basis function coefficients to muscle lengths. In this case, we can group muscles for each joint and create a Jacobian for each group. The Jacobian for muscle

group $\vec{X_j}$ would be represented as J_{α_j} and defined as,

$$J_{\alpha_j}(\vec{\alpha}) = \begin{bmatrix} \frac{\partial x_1}{\partial \alpha_1} & \cdots & \frac{\partial x_1}{\partial \alpha_p} \\ \vdots & \ddots & \vdots \\ \frac{\partial x_l}{\partial \alpha_1} & \cdots & \frac{\partial x_l}{\partial \alpha_p} \end{bmatrix}. \tag{5.1}$$

For each group we pick out p coefficients that would be used for the reconstruction of the muscles in that group. This would ensure that we have a fixed set of variables that would be used to reproduce that muscle group. The muscle length is defined as,

$$x(t) = \sum_{\gamma \in \Gamma_i} \alpha_\gamma \, \phi_\gamma(t) + R^{(M)},$$

where, $\Gamma_i \subset \Gamma$ is the minimal set of basis functions used to reproduce that muscle signal. For a muscle group, X_j corresponding to angle α_j, the set of basis functions used in reproducing any of the muscles in the group is given as Γ_j. For a muscle x_i, if we ignore the residual $R^{(M)}$, we can say $\dfrac{\partial x_i(t)}{\partial \alpha_j} = \phi_j(t)$, since each $\phi(t)$ is independent of α. This implies, if ith muscle includes the jth basis function in its reproduction then,

$$\frac{\partial x_i}{\partial \alpha_j}(t) = \phi_j(t),$$

and, if the ith muscle does not include the jth basis function in its reproduction then, $\frac{\partial x_i}{\partial \alpha_j}(t) = 0$. Thus J_α is computed as,

$$J_{\alpha_j}(\vec{\alpha})_t = \begin{bmatrix} \phi_1(t) & \cdots & \phi_p(t) \\ \vdots & \ddots & \vdots \\ \phi_1(t) & \cdots & \phi_p(t) \end{bmatrix},$$

where, entry (i, j) would be 0 if jth basis function is not a part of the reconstruction of the ith muscle.

(a) Subject placing a forehand stroke

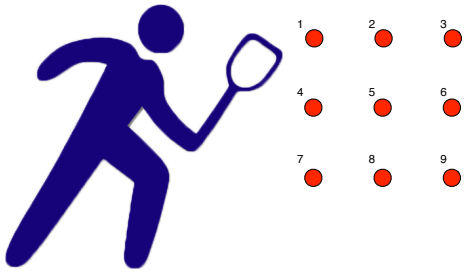

(b) Grid of points to which strokes were measured

Figure 5.5: Experimental setup for capturing array of strokes to a grid of stationary balls.

Computing J_θ would be easy - if the jth joint is a rotational joint with a single degree of freedom, the joint angle is a single scalar θ_j. Let $\mathbf{p}_j$ be the position of the joint, and let $\mathbf{v}_j$ be a unit vector pointing along the current axis of rotation for the joint. In this case, if angles are measured in radians with the direction of rotation given by the right-hand rule and if the ith end effector is affected by the joint, then the corresponding entry in the Jacobian is

$$\frac{\partial s_i}{\partial \theta_j} = \mathbf{v}_j x (s_i - \mathbf{p}_j),$$

and 0, if the end effector is not affected by the jth joint.

A small change in the end effector can, thus, be related to the coefficients as, $\Delta s_i = J_\theta J_X J_\alpha \Delta\alpha$. Taking the inverse we obtain,

$$\Delta\alpha = J_\alpha^{-1} J_X^{-1} J_\theta^{-1} \Delta s_i.$$

In this research work, we perform an exploratory analysis of applying

the Jacobian transformation to extract new trajectories. We perform a pilot study of this framework by focusing on Equation 5.1. We captured tennis swings from a single subject hitting a grid of 9 points using a stationary tennis stand (see Figure 4.4b). The subject was instructed to always start from the same point with the target ball moved across the grid (see Figure 5.5). We computed the muscle trajectories for three muscles of the arm: biceps brachii long head, deltoids, and triceps brachii. These trajectories were encoded using PMP as coefficients of Gabor functions.

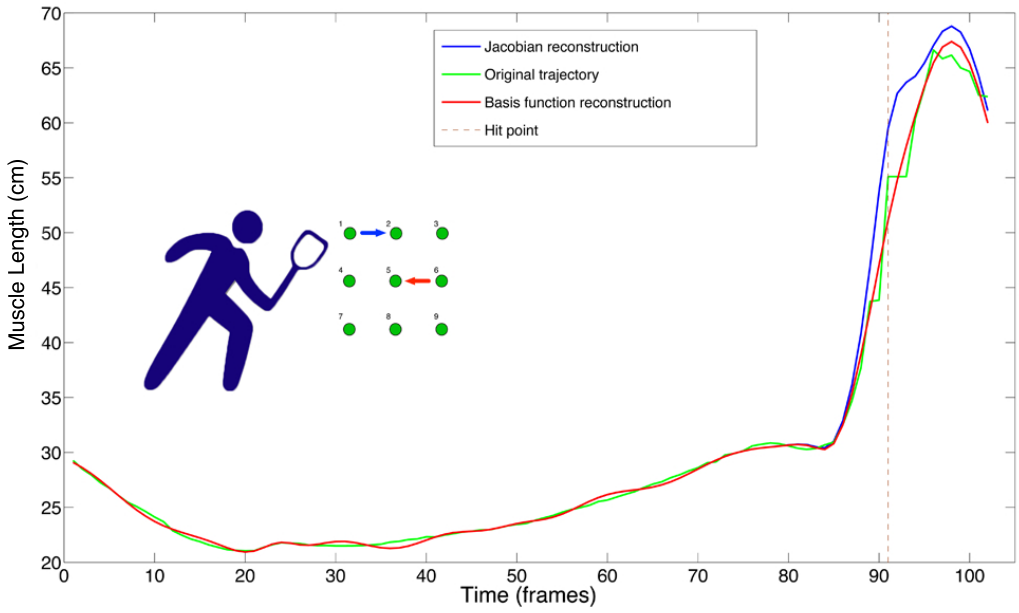

Figure 5.6: Preliminary result for computing new coefficients for a new hit point using Jacobians that relate end points to muscle length parameters. The green curve is the captured trajectory for a swing at point 5 and red curve is the basis function reconstruction. The blue curve is the reconstruction from the new coefficients (same basis set as before) computed from the Jacobian of the hit point. The vertical displacement at the hit point shows that the joint has been moved in a direction that displaces the racquet towards the new hit point.

Figure 5.6 illustrates the result from our preliminary simulation of using the coefficient Jacobian technique that related the change in endpoint to the change in muscle length of a single relevant muscle. The coefficients computed from a trajectory to the center point (point 5) were related to the change in muscle length using Equation 5.1. This allowed us to compute the change in coefficients for a small change in the end point of the muscle length trajectory. In Figure 5.6 we can see that the change in hit point can be projected back in to the coefficients of the basis functions coding a muscle length appropriately transforms the original trajectory (red) into one closer to the new hit point (blue).

This study explores the capability of the Jacobians to generalize the pre-learned movements to produce new movements in the same vicinity. The use of a gradient for trajectories was explored by Torres and Zipser [2002] but that strategy used a local temporal gradient of the motor trajectory. Sentis et al. [2010] have effectively used Jacobian constructs to create optimal controllers for humanoid robots. This work differs from that framework since we employ Jacobians that not only project onto the end-point of the trajectory but rather affect the whole trajectory due to presence of the basis functions.

Chapter 6

Related Work

This dissertation introduces a novel method for creating a code for human movements that employs ideas from sparse coding in signal representation and motor primitives in human and humanoid research. This chapter provides an overview of work by other scholars that either shares the same objective as our research work or employs similar ideas. Section 6.1 provides an overview of how effective sparse coding has been in vision and audition. Section 6.2 provides the progress made in understanding human motor control in the scope of motor primitives. Finally, section 6.3 summarizes the computational side of motor primitives, and illustrates some of the robotic constructs using such primitives.

6.1 Efficient neural codes

The primary motivation for this research work has been the seminal work by Olshausen and Field [1996] and Smith and Lewicki [2006]. Olshausen and Field [1996] demonstrated that neurons in the visual cortex encode both the location and the spatial frequency of visual stimuli. It has been shown that maximizing statistical independence or sparseness of visual representations yields spatial receptive field properties similar to those of cortical neurons. They have shown how natural image sequences can be described in terms of a superposition of meaningful sparse, spatiotemporal events (Figure **??**).

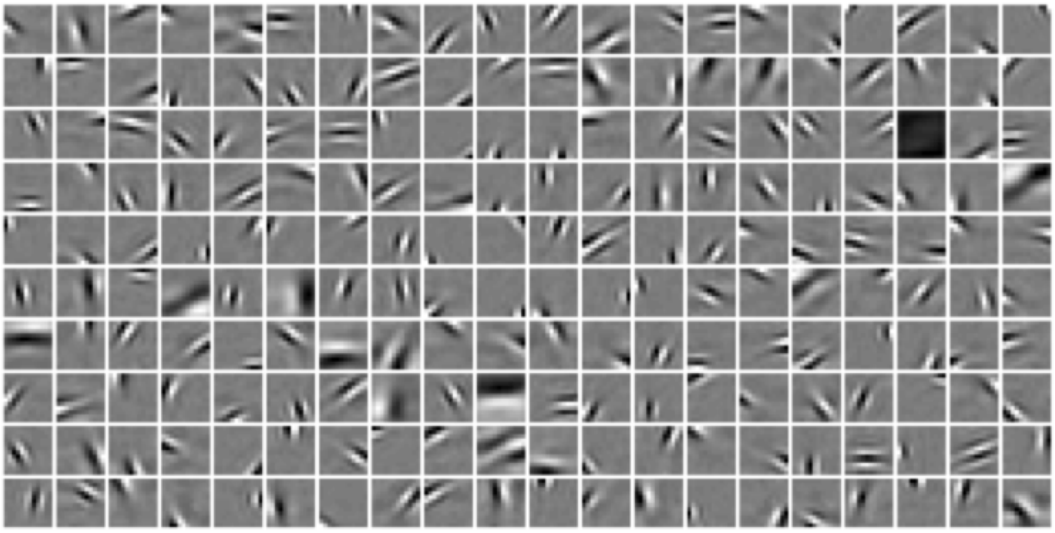

Figure 6.1: Basis functions learned from static natural images. Shown is a set of 200 basis functions which were adapted to pixel image patches [see Olshausen and Field, 1997, for more details].

Lewicki and Sejnowski [2000] showed that when efficient coding is applied to different ensembles of natural sounds, the timefrequency tiling patterns that emerge are strikingly diverse. For environmental sounds (such as crackling twigs), one obtains timefrequency windows similar to a wavelet, whereas for animal vocalizations (monkey coos), one obtains a tiling pattern similar to the Fourier transform. Speech, which contains a mixture of temporal and frequency cues, gives rise to an intermediate tiling pattern, somewhere between a Gabor and a wavelet; the temporal accuracy increases with frequency, but to a lesser extent than with wavelet filters. As Lewicki shows, a close match is obtained with a 2:1 mixture of environmental to animal sounds. Interestingly, this pattern is similar to what has been observed physiologically in cat auditory nerve fibers, and it also bears similarity to the auditory filters that have been characterized psychophysically in humans and

other animals.

6.2 Perspectives on spinal motor systems

It has long been known that spinal motor systems are capable of producing a wide range of motor behaviors when isolated from the rest of the nervous system. This fact, together with the descriptions of many interneuronal pathways within the spinal cord and their elaborate interactions, further indicate that the spinal cord cannot be viewed as a simple relay of supraspinal motor commands to the periphery. Because of its obvious importance, the organization of movement by the spinal cord has been investigated by many researchers.

Bizzi et al. [2000] hypothesize that movements mediated by the spinal cord are based on the combination of a small number of behavioral units. In this hypothesis, the flexible combination of a small set of spinal modules is proposed to be used by the nervous system to produce a wide range of movement in a simple manner. Experimental studies on spinalized frogs, turtles, rats and cats have led to the conclusion that the premotor circuitries within the spinal cord are organized into such a set of distinct modules.

D'Avella et al. [2006] characterized the spatiotemporal organization of the muscle patterns for fast-reaching movements. They recorded electromyographic activity from up to 19 shoulder and arm muscles during point-to-point movements between a central location and 8 peripheral targets in each of 2 vertical planes. They used matching pursuit to identify a set of time-varying muscle synergies, i.e., the coordinated activations of groups of muscles with specific time-varying profiles.

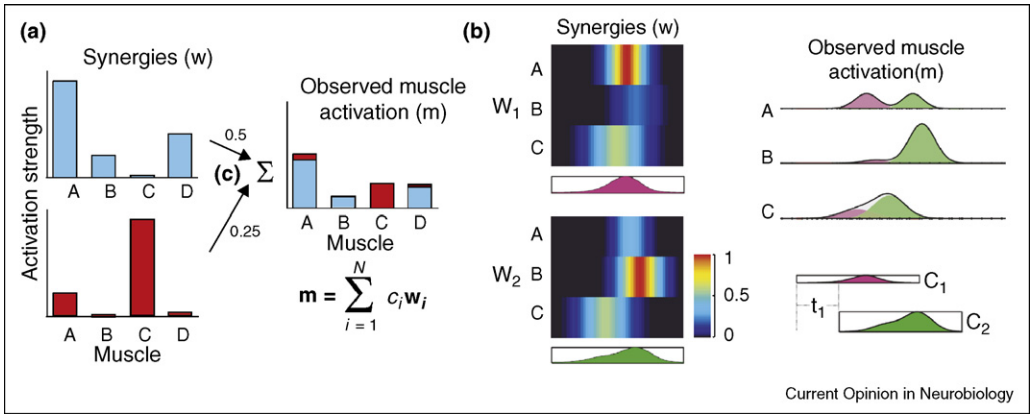

Figure 6.2: Schematic representation describing the muscle synergy hypothesis. (a) A schematic representation for synchronous synergies. Two synergies (w) are scaled (c) and summed to produce the observed pattern of muscle activations (m). These synchronous synergies are fully described by the balance of activation across the muscles in each synergy: any temporal structure is specified by the scaling coefficients (c). (b) A schematic illustrating time-varying synergies. Two time-varying synergies (w) are shown. Each synergy specifies a weighting coefficient for one of the three muscles, indicated by the color of the bar and a temporal profile for these weightings. An observed pattern of muscle activations is created by scaling each synergy (c), temporally shifting them (t), then adding them together linearly. Figure reproduced from [Tresch and Jarc, 2009]

Ivanenko et al. [2005] have shown using Factor Analysis that muscle activity during human locomotion is driven by a few (approximately five) temporal activation components. Each activation component describes a short period of synchronous activation or relaxation of a particular set of muscles, and it represents a characteristic timing rather than a characteristic muscle synergy associated with each movement component. They also illustrated that the coordination of locomotion with various voluntary tasks was accomplished by combining activation timings that were associated separately with the voluntary task and locomotion. Activation associated with the voluntary

tasks was either synchronous with the timing for locomotion or had additional activations not represented in the basic locomotion timing. This suggests presence of motor programs in the spinal cord that describe the locomotion in general with various supra-spinal elements involved in voluntary adaptions.

6.3 Optimal Motor Behavior

A computational theory of motor behavior might involve a model that formalizes the actors goals as mathematical criteria and searches for the actions that optimize the criteria. An optimal analysis of the optimal actions could then derive the motor synergies. Synergies discovered in this way would be "optimal" in the sense that they arise from a computational theory of optimal motor behavior. It is important to keep in mind, however, that motor primitives and synergies that are described in this dissertation arise from optimal analysis of peoples actions and are not necessarily the same ones as would arise from a computational theory of motor behavior.

Todorov and Jordan [2002] introduced a novel idea of motor coordination, based on optimal feedback control, bringing together a number of key ideas that have stimulated motor control research since the pioneering work of Bernstein. They postulate that optimal feedback controllers resolve redundancy online by obeying a minimal intervention principle: make no effort to correct deviations away from the average behavior unless those deviations interfere with task performance (example in Figure 6.3).

Schaal [2003] have formulated a comprehensive framework for modular motor control based on a recently developed theory of dynamic movement primitives (DMP). DMPs are a formulation of movement primitives with autonomous nonlinear differential equations, whose time evolution creates

smooth kinematic control policies. They have employed model-based control theory to convert the outputs of these policies into motor commands. By means of coupling terms, on-line modifications was incorporated into the time evolution of the differential equations, thus providing a rather flexible and reactive framework for motor planning and execution. Ijspeert [2008] and Schaal [2003] have demonstrated how DMPs can be used to model both rhythmic and discrete movements.

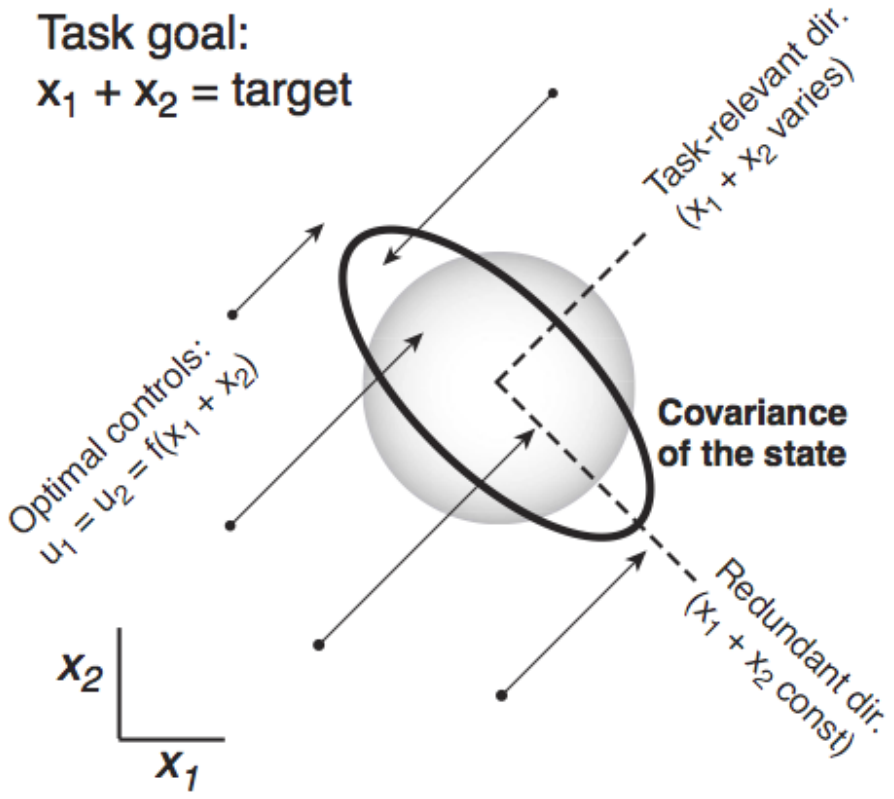

Figure 6.3: Minimal intervention principle. Illustration of the simplest redundant task, reproduced from [Todorov and Jordan, 2002]. x_1, x_2 are two uncoupled state variables, each driven by a corresponding control signal u_1, u_2. The task is to maintain $x_1 + x_2 = target$ and use small controls. The optimal u_1, u_2 are equalto a function that depends on the task-relevant feature $x_1 + x_2$ but not on the individual values of x_1, x_2. Thus u_1 and u_2 form a motor synergy. Such a control law can reduce variance in the redundant direction as compared to the optimal control law, but only at the expense of increased variance in the task-relevant direction. [See Todorov and Jordan, 2002, for technical details].

Chapter 7

Conclusion and Future Work

Humans are able to adapt their movements to almost any new situations in a robust, seemingly effortless way. To explain both this adaptivity and robustness, a promising perspective is the modular approach to movement generation: Movements result from combinations of a finite set of stable motor primitives organized at the spinal level. There is still an evolving research field on building a formal framework for representing the communication between cortical and spinal regions to employ these motor primitives. In this research, we present such a formalism by encoding the temporal signals of muscle movements as a time-shiftable, kernel representation. We show in our research work that a relative small library of oscillators, commonly called in motor control literature as central pattern generators (CPGs), can code complex muscle changes in walking at different speeds and inclines. The ultimate goal of this research work is to build a complete library of CPGs that can efficiently code all natural human movements. This work is the first step towards that goal.

To summarize the contributions of the dissertation, in chapter 2, we introduced the notion of motor primitives and the current applications in robotic systems. Solving the complex problem of redundancy in a challenge and involves building an accurate model of the body and coordinate vast number of degrees of freedom. A viable solution is to treat the control problem

as a hierarchy - lower level control structures like muscles can be controlled using a short-loop feedback mechanism by the spinal regions. These could be done using primitives that describe the movement trajectory as a linear superposition of oscillators. The actual control signal would then be computed as a difference between the actual trajectory and the desired trajectory.

Chapter 3 provided the theoretical framework on how to build movement primitives. Previous studies had used natural stimuli to learn an appropriate representation set to encode signals. We employed a similar strategy to encode the trajectories followed by muscles during natural human movements. We represented muscle length as a superposition of non-linear functions, collectively placed in a dictionary. Matching pursuit is a greedy algorithm that encodes a signal by projecting it to such a dictionary and picking the highest projection as an encoding coefficient. The residual is then projected back to the dictionary to get another coefficient, the process repeating till the residual is smaller than a threshold. We developed a new method based on matching pursuit that applies this process on a parameterized dictionary. Matching pursuit optimizes its projection by backprojecting the error residual back into the dictionary, specifically the atom chosen in current projection. We replace this process by a gradient search algorithm that updates the parameter of the current chosen atom in the direction of lowest error.

We captured data from eight human subjects that included walking on a treadmill at different speeds and varying inclines. In chapter 4 we presented results on applying our sparse code model to represent walking. We discussed the efficiency of the code in representing captured movements, and compared it to using Fourier transformation. We also discussed it efficacy in extracting

the differences in the subtle changes involved in walking at different speeds and inclines. Finally, we looked at an experiment to understand the adaptations involved in walking with a change in limb dynamics.

In chapter 5 we discussed two ways in which we can extend this framework of sparse coding. Dating at least back to the work of Sherrington [Sherrington, 1910], several researchers have proposed that the CNS produces movement by combining small groups of muscles. This hypothesis has been formulated in several different ways, but has been most recently expressed in terms of a group of muscles, also referred to as a muscle synergy. We showed that there is high correlation in lower limb muscle length changes while walking, and how we can combine the encoding for muscles in a synergy during training to reduce the dimensionality even further. This ensures that we reuse resources in cases where there is redundancy and overlap in function between muscles. Further, after learning the coefficients for a particular trajectory, it would require to generalize and reuse the same coefficients to achieve a different, but related trajectory. We explored the idea of using a Jacobian to relate a change in the trajectory to changes in the coefficient that encodes the trajectory. We formulated the mathematical foundation that can be used to apply such a generalization and performed pilot analysis to show promising results.

The research work presented in this thesis touches on aspects of motor control and signal representation. As with any research, while answering some questions, it raises further important questions. Below, we briefly summarize the most important ones.

Motor primitives in more complex tasks

This dissertation focuses on walking as the primary movement to encode.

It would not be difficult to extend this to repertoire of movements. The basis functions that are learned over a distribution of movements would more accurately represent human movement structure. Further, we focus on using Gabor as our representative parametric-function. The algorithm though is a general parametric search process, and can be used with any dictionary that can be represented in such a parametric form.

Control signals for muscles

The coefficient obtained from the analyses here only represent half the picture. We still need to transform a desired trajectory encoded by the coefficients to an actual signal sent to the muscles. We believe that "threshold control" Latash [2010] theories are appropriate to compute a muscle control signal from a set of coefficients. Appendix B provides an overview of threshold control and a specific form called 'Equilibrium Point Hypothesis'.

Incorporating dynamics

The SIMM muscle simulation system allows the estimation of muscle activations, but the central issue is that even if the joint torques are determined, their division amongst the component muscles is undetermined. The modeler must supply their own additional constraints to derive activation estimates, but even with these, the computation is laborious and can be unreliable. Cooper and Ballard [2012] developed a novel joint torque recovery system that rapidly recovers joint torques. The method uses the Phasespace marker information as forcing functions in a physics equation solver (ODE) so that the driven joints are constrained to produce good torque estimates. It is, however, unclear how these joint torques can be translated to compute muscle force activation signals. Small electrical currents are generated by muscle fibers prior to the production of muscle force. These currents are generated by the exchange

of ions across muscle fibre membranes, a part of the signaling process for the muscle fibers to contract. The signal called the electromyogram (EMG) can be measured by applying conductive elements or electrodes to the skin surface, or invasively within the muscle. As discussed in chapter 6, EMG measurements have been used by other researchers to extract motor primitives from human movements. We could add to this literature by exhibiting a encoding strategy that translates joint torques obtained using ODE to EMG primitives in muscles. That would provide a general purpose, hierarchical motor primitives model that can be used in dynamical environments.

Appendices

Appendix A

Description of muscles used in walking simulation

This appendix chapter provides details on the lower limb muscles involved in hip and knee movements that were used in the simulations in this research work [see Zuckerman, 1961, for a complete review].

Muscle	Origin	Insertion	Action
Gracilis	inferior ramus of pubis	upper part of tibia on medial surface	adducts thigh and flexes leg
Adductor longus	body of pubis	posterior surface of femur	adducts thigh; assists in lateral rotation
Adductor brevis	inferior ramus of pubis	posterior surface of femur	adducts thigh; assists in lateral rotation
Adductor magnus	inferior ramus of pubis; ramus of ischium	posterior surface of shaft of femur	adducts thigh; hamstring part extends thigh

Table A.1: Muscles of Medial Compartment of Thigh

Muscle	Origin	Insertion	Action
Sartorius	anterior iliac spine	upper medial surface of tibia	flexes, abducts, rotates thigh
Iliacus	iliac fossa	lesser trochanter of femur	flexes thigh on trunk; helps in sitting up
Psoas	12th thoracic body	lesser trochanter of femur along with iliacus	flexes thigh on trunk
Pectineus	superior ramus of pubis	upper end of femur	flexes and adducts thigh
Quadriceps femoris, Rectus femoris	anterior iliac spine	quadriceps tendon into patella	extension of leg
Vastus lateralis	upper end of femur	quadriceps tendon into patella	extension of leg
Vastus medialis	upper end and shaft of femur	quadriceps tendon into patella	extension of leg
Vastus intermedius	shaft of femur	quadriceps tendon into patella	extension of leg

Table A.2: Muscles of Anterior Compartment of Thigh

Muscle	Origin	Insertion	Action
Biceps femoris	long head from ischial tuberosity; short head from shaft of femur	head of fibula	flexes and laterally rotates leg
Semi-tendinosus	ischial tuberosity	upper part medial surface of shaft of tibia	flexes and medially rotates leg
Semi-membranosus	ischial tuberosity	medial condyle of tibia	flexes and medially rotates leg
Adductor magnus	ischial tuberosity	adductor tubercle of femur	extends thigh

Table A.3: Muscles of Posterior Compartment of Thigh

Muscle	Origin	Insertion	Action
Gluteus maximus	outer surface of ilium	iliotibial tract and gluteal tuberosity of femur	rotates thigh and extends knee joint
Gluteus medius	outer surface of ilium	greater trochanter of femur	abducts thigh, tilts pelvis when walking
Gluteus minimus	outer surface of ilium	greater trochanter of femur	abducts thigh, medially rotates thigh
Piriformis	anterior surface of sacrum	greater trochanteric fossa	lateral rotator of thigh
Superior gemellus	spine of ischium	greater trochanteric fossa	lateral rotator of thigh
Inferior gemellus	ischial tuberosity	greater trochanteric fossa	lateral rotator of thigh

Table A.4: Muscles of Gluteal Region

Appendix B

Threshold Control

This appendix chapter introduces the idea of 'theshold control' and provides the control strategy that we believe to be the right complement to motor primitives. Most of the section is extracted from Latash [2010]; Ostry and Feldman [2003]; Latash [2008]; Feldman [2006] and is included here for completion.

In the force control formulation, desired movement trajectories are planned first in terms of spatial coordinates and their derivatives, and then transformed into required forces and torques. In order to compute torques, the system uses an internal representation of dynamical equations of motion of the body interacting with the environment. The hypothetical computational process, which may be realized by a neuronal network, is called inverse-dynamics because it generates values of torques based on kinematics and thus inverts the input/output relationships inherent in actual (direct) dynamical laws in which torques cause changes in kinematics rather than the other way around [Hogan, 1984]. The main idea of the force control model is that the control level of the nervous system directly deals with or calculates forces required for the production of voluntary movements. Kinematic variables can be measured directly using one of numerous recording techniques whereas inverse-dynamics computation remains practically the only method of deriving muscle torques especially in studies of multi-joint movement. Inverse-dynamics

was used initially to characterize the forces associated with different patterns of locomotion [see Winter, 1984, for review]. Hollerbach and Flash [1982] hypothesized that movement production by the nervous system may involve similar computations, consisting of a transformation from endpoint to joint coordinates and then an inverse computation of joint torques based on the equations of motion of the arm. The term internal model is now also widely used in studies of motor control in a more general, metaphorical sense to imply adjustments to the neural activity that are carried out as a result of previous learning or adaptation, rather than in the specific sense implied in the force control formulation in which learning and adaptation are based on internal reproductions of systems input/output relationships.

An alternative approach to the control of human movement starts not with the control theory and laws of classical mechanics but with the design of the human body, in particular its central nervous system. Such systems can be controlled only by setting their parameters, while their output emerges given the parameters and the interaction with the environment that proceeds according to the laws of physics. This approach to voluntary movements has been developed over the past half-a-century [reviewed in Kugler and Turvey, 1986; Latash, 2008]. Typically, these systems are divided into two interrelated aspects: 'control' (the nature of neural variables that are manipulated to produce movements) and coordination (co-variation of the outputs of elements in a multi-element system). In this document, we focus on the control aspect of the movement, and specifically the equilibrium-point hypothesis.

To clarify the notion of control that may be applied to biological systems we need to consider very general characteristics of natural laws. These laws express the relationships between certain variables called state variables

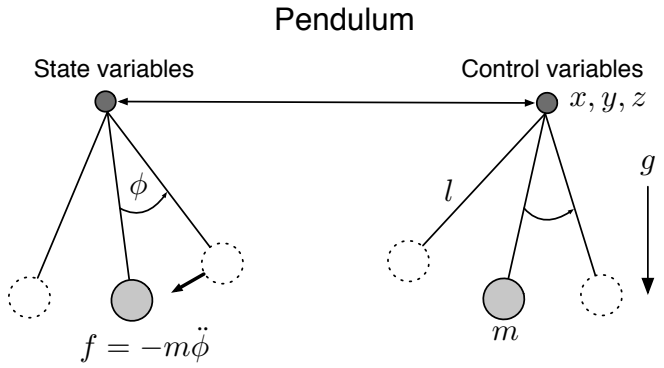

Figure B.1: Example of state and control variables. The force (f) and kinematic variables (ϕ and its derivatives) are the state variables (SVs). The coordinates of suspension point (x, y, z), the mass (m), the length (l), and the direction of gravity (g) are the parameters or control variables (CVs) independent of the SVs.

(SVs; e.g., forces and kinematic variables in laws of mechanics). Constrained by natural laws, SVs, cannot be specified directly by the nervous system. The nervous system, on contrary, specifies motor behavior using parameters, called control variables (CVs). Figure B.1 shows the difference between SVs and CVs in a simple physical system a pendulum (a mass on a rope). In a steady state the pendulum would be in an equilibrium. However, it is not the forces or kinematic variables that directly determine where in the force-position space would this equilibrium be achieved, but the parameters of the pendulum. Even the frequency of oscillation would be determined by the length of the rope. By changing the parameters, for example, the coordinates of the suspension point in a pendulum, one can transfer the oscillations to a new location in space. No knowledge of the natural law that governs this motion is necessary to produce a movement. Instead, it can be relied on general experience and memory. With the recognition that control of actions implies changes in parameters

of natural law one needs to identify the specific parameters that the nervous system modifies to control posture and movement of the body. Threshold control theory and equilibrium point hypothesis explores explores the nature of such parameters.

B.1 Equilibrium-Point Hypothesis

The Equilibirum-Point hypothesis (EPH) [Feldman, 1966, 1986] quantifies physiological variables that are used by the central nervous system as control variables. According to the EP-hypothesis, central control signals change the threshold of activation of alpha-motoneurons to afferent signals related to muscle length (threshold of the tonic stretch reflex, λ) by subthreshold depolarization of the alpha-motoneurons. Central signals are not the only ones contributing to λ, which also changes with muscle velocity (because of the velocity-sensitivity of muscle spindle endings), signals from sensory receptors in other muscles, and history of activation [Feldman and Latash, 2005].

Let's focus on the control of a single muscle to understand EPH in detail. A dependence between muscle force and length was found during slow muscle stretch in an experiment, when there are no changes in signals from the brain. This was achieved in animal experiments by transecting all the pathways leading from the brain to the spinal cord and placing a stimulator at the spinal end of the cut fibers [Matthews, 1959]. In human experiments, similar results were obtained, when a person was asked "not to interfere voluntarily" [Feldman, 1966]. Let us imagine that a muscle at a relatively short length is completely relaxed, that is, it does not show signs of electrical activity. Then, the muscle would resist an externally imposed stretch by generating opposing forces due to its (and also the tendon's) peripheral

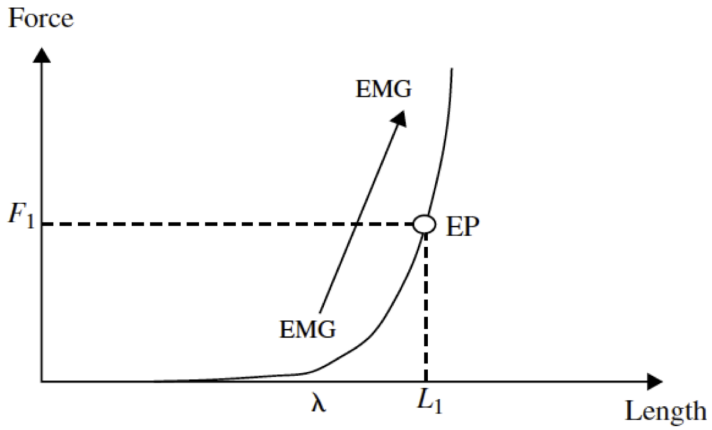

Figure B.2: Slow stretch of a muscle leads to an increase in its force due to passive properties of the "muscle + tendon" complex. At a certain length, the muscle shows signs of activation. This length is called the threshold of the tonic stretch reflex (λ). If a muscle acts against a constant external load (F_1), it has only one equilibrium length (L_1) that corresponds to its active force exactly equal to F_1. The combination of muscle force and length, at which it is at an equilibrium, is called the equilibrium point (EP). [Reproduced from Latash, 2008].

elasticity. At some value of the muscle length, the muscle will show signs of increasing electrical activity. This length value (λ) was termed the *threshold of the tonic stretch reflex*.

If we continue to stretch the muscle beyond λ, it will oppose the stretch more vigorously, as a much stiffer spring. In Figure B.2, this is reflected in the much steeper forcelength curve after λ compared to the curve before λ. Let us stop stretching the muscle at a certain length L_1, at which it generates a force F_1. This combination of length and force values can be referred to as an equilibrium-point (EP) of the system: "the muscle with its reflex connections and the external force". If a small, transient change in the external force moves the muscle away from the F_1, L_1 point, the muscle will return as soon as the

transient force change is over. Note that for a given external force and fixed λ, there is only one muscle length value, at which the muscle can be in an equilibrium. We can now define the tonic stretch reflex as a neural mechanism that ensures a particular relation between muscle length and active muscle force. This definition makes this reflex a major posture-stabilizing mechanism.

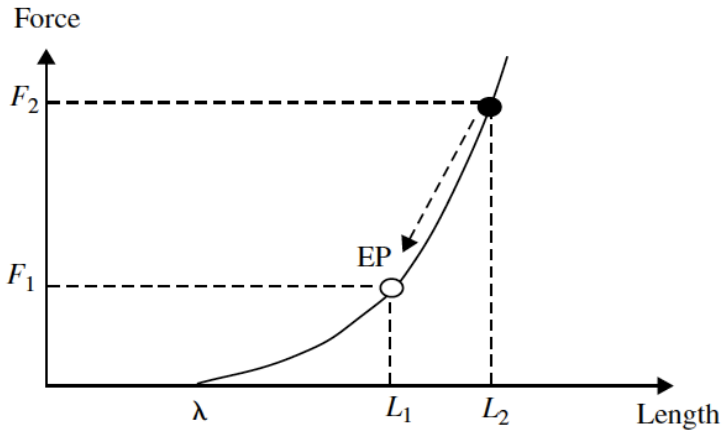

Figure B.3: Posture stabilizing using EP points. If a muscle is at an equilibrium point (EP), an external force can stretch it to a new length (L_2) corresponding to a new force level (F_2). However, when the force is removed, the muscle will return to EP (posture-stabilizing mechanism). If the controller wants the muscle to stay at this new length, its has to deal with the posture-stabilizing mechanism. [Reproduced from Latash, 2008].

If an external factor moves the muscle from its EP to a new length value, and if the force-length curve (IC) remains unchanged, then the new length value, for example, L_2 in Figure B.3, would correspond to a different force produced by the muscle, F_2. The difference between this force and the original external force F_1 will tend to move the muscle back to its equilibrium position. Note that EP is not a value of muscle length but a combination of muscle length and force values. Posture-stabilizing mechanisms ensure stability of EP under

transient external force perturbations. Two types of movement are possible within this scheme, passive that follow change in L without a change in λ, and active when λ is changed by the controller. In either case, the original EP shifts to a new location that may involve a change in length, force, or both.

B.2 Muscle Control

Voluntary muscle control is associated with three distinct time patterns of important variables. First, the time profile of the control variable, $\lambda(t)$ may be viewed as the *control trajectory*. Second, for each λ (given an external condition), there is an instantaneous EP a combination of muscle length and force that would have been observed if the control process stopped and the system were given time to reach an equilibrium state. Instantaneous EP is typically not directly observable, in particular because of the inertial properties of the system. A time sequence of EPs forms an *equilibrium trajectory* of the system that can be described with two variables $x_{\mathrm{EP}}(t); F_{\mathrm{EP}}(t)$, i.e. in units of displacement and force. And finally, there is an *actual trajectory* that can also be described in both units of displacement and force.

Within the EP-hypothesis, movements may result from two different sources. On the one hand, a movement may be a consequence of a change in the external load, while the person does not change the voluntary command to the muscle. A change in the load while keeping the command constant results in a new combination of muscle force and length along the same IC, that is, a movement. One may address such a movement as "involuntary". On the other hand, a voluntary shift in λ can also lead to a movement. For example, in Figure B.4, a shift from λ_1 to λ_2 is expected to lead to a movement from L_1 to L_2, if the external load stays constant at F_1. On the other hand, if a movement

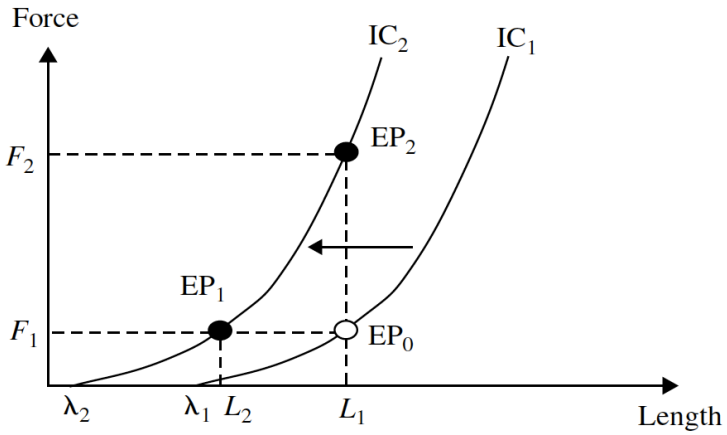

Figure B.4: According to EPH, movement and force generation are different peripheral consequences of the same control process. A shift of the control variable λ leads to a shift of the invariant characteristic (IC). If the muscle acts against a constant external force, a movement will occur from the original length L_1 to a new length L_2. If a muscle presses against a stop (isometric conditions), the same shift of λ will lead to a change in the muscle force from F_1 to F_2. [Reproduced from Latash, 2008]

is blocked by an external stop, the same change in λ will lead to a change in the muscle force without a movement. So, within the λ-model, voluntary movements and voluntary force changes are different peripheral consequences of basically the same central control processes. Commonly, voluntary motor actions are associated with a shift in λ, while the external load changes as well, such that both factors influence the movement.

It is easy to generalize it for a system of two muscles that act at a joint and produce joint torques in opposite directions, for example a flexor and an extensor muscle. Figure B.5 illustrates ICs for two such muscles with opposing actions. It uses torque and angle(rather than force and length), that are more appropriate to describe rotational actions. Each muscle is controlled with its own command variable, λ_{FL} for the flexor and λ_{EX} for the extensor. These

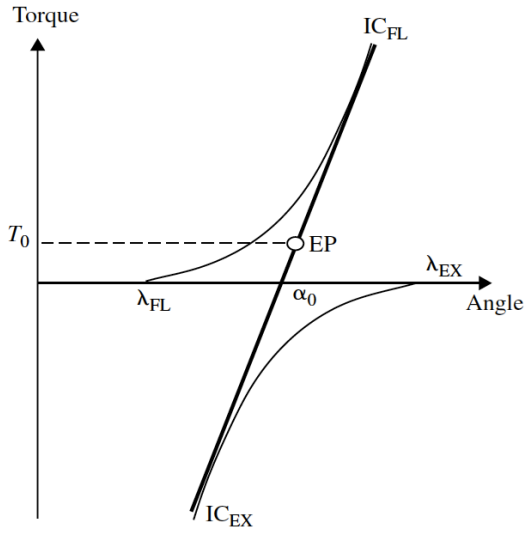

Figure B.5: Invariant characteristics (IC_{FL} and IC_{EX}) of a flexor and extensor muscle can be drawn on a torque-angle plane. The behavior of the joint will be defined by the algebraic sum of the two characteristics (the thick, straight line). Its equilibrium point will be defined by both the position of this line and the external torque (T_0). [Reproduced form Latash, 2008]

commands define the positions of the ICs for each muscle. A pair of such characteristics define an overall joint characteristic shown by the bold line. Equilibrium state of the joint and its mechanical behavior will also depend on the external torque.

Bibliography

Phasespace inc, optical motion capture systems. URL `http://www.phasespace.com`.

Shadow robot company. URL `www.shadowrobot.com`.

Vicon inc, motion capture systems. URL `http://www.vicon.com`.

Afsheen Afshar, Gopal Santhanam, Byron M. Yu, Stephen I. Ryu, Maneesh Sahani, and Krishna V. Shenoy. Single-trial neural correlates of arm movement preparation. *Neuron*, 71:555–564, 2011.

T. Arakawa and T. Fukuda. Natural motion generation of biped locomotion robot using hierarchical trajectory generation method consisting of ga, ep layers. In *Proceedings of the IEEE International Conference on Robotics and Automation*, pages 211–216, 1937.

Yoseph Bar-Cohen. Electroactive polymers as artificial muscles - capabilities, potentials and challenges. *Robotics and Space*, 2000.

E. Bizzi, S. Giszter, G Loeb, and F. A. Mussa-Ivaldi. Modular organization of motor behavior in the frog's spinal cord. In *Trends in Neurosciences*, volume 18, pages 442–446, 1995.

E. Bizzi, V. Cheung, A. d'Avella, and M. Tresch. Combining modules for movement. In *Brain Research Reviews*, volume 57, pages 125–133, 2008.

Emilio Bizzi, Matthew Tresch, and Andrea d'Avella. New perspectives on spinal motor systems. *Nature Reviews*, 1:101–108, 2000.

J. Buchli, F. Stulp, E. Theodorou, and S. Schaal. Learning variable impedance control. *International Journal of Robotics Research*, 30:820–833, 2011.

Scott Chen, David Donoho, and Michael Saunders. Atomic decomposition by basis pursuit. *SIAM Journal of Scientific Computing*, 20(1):33–61, 1999.

J. M. Cooper and D. H. Ballard. Physically-based humanoid animation from human demonstration data. In *SIGGRAPH 2012*, submitted 2012.

Ingrid Daubechies. Time-frequency localization operators: a geometric phase space approach. *IEEE Transactions on Information Theory*, 34:605–612, 1988.

Andrea d'Avella, Allessandro Portone, and Laure Fernandez. Control of fast-reaching movements by muscle synergy combinations. *Journal of Neuroscience*, 26:7791–7810, 2006.

Geoff Davis. *Adaptive Nonlinear Approximations*. PhD thesis, New York University, 1994.

Scott Delp. *Surgery Simulation: A Computer Graphics System to Design and Analyze Musculoskeletal Reconstructions of the Lower Limb*. PhD thesis, Stanford Universiry, 1990.

Scott Delp and Peter Loan. A graphics based software system to develop and analyze models of musculoskeletal structures. *Computational Biology Medicine*, 25(1):21–34, 1995.

H. Elftman. The measurement of the external force in walking. *Science*, 88: 152–153, 1938.

Anatol Feldman. Functional tuning of the nervous system with control of movement or maintenance of a steady posture. ii. controllable parameters of the muscle. In *Biophysics*, volume 11, pages 565–578, 1966.

Anatol Feldman. Once more on the equilibrium-point hypothesis (lambda model) for motor control. *Journal of motor behavior*, 18(1):17–54, March 1986. ISSN 0022-2895. URL `http://view.ncbi.nlm.nih.gov/pubmed/15136283`.

Anatol Feldman and Mark L. Latash. Testing hypotheses and the advancement of science: Recent attempts to falsify the equilibrium-point hypothesis. In *Experimental Brain Research*, volume 161, pages 91–103, 2005.

Anatol G. Feldman. *The Nature of Voluntary Control of Motor Actions*, chapter 1, pages 3–8. Springer, 2006.

S. Giszter, F. A. Mussa-Ivaldi, and E. Bizzi. Convergent force fields organized in the frog's spinal cord. In *Journal of Neuroscience*, volume 13, pages 467–491, 1993.

M. S. A. Graziano and T. N. Aflalo. Mapping behavioral repertoire onto the cortex. *Neuron*, 56:239–251, 2007.

S Grillner. Biological pattern generation: The cellular and computational logic of networks in motion. *Neuron*, 52:751–766, 2006.

Neville Hogan. An organizing principle for a class of voluntary movements. In *The Journal of Neuroscience*, volume 4, pages 2745–2754, 1984.

J. M. Hollerbach and T. Flash. Dynamic interactions between limb segments during planar arm movements. *Biological Cybernetics*, 44:67–77, 1982.

A. J. Ijspeert, A. Crespi, D. Ryczko, and J. M. Cabelguen. From swimming to walking with a salamander robot driven by a spinal cord model. *Science*, 315:1416–1420, 2007.

Auke Jan Ijspeert. Central pattern generators for locomotion control in animals and robots: A review. In *Neural Networks*, volume 21, pages 642–653. Elsevier, 2008.

Yuri Ivanenko, Germana Cappellini, Nadia Dominici, Richard E. Poppele, and Francesco Lacquaniti. Coordination of locomotion with voluntary movements in humans. *Journal of Neuroscience*, 25(31), 2005.

Hughlings J Jackson. On the comparative study of disease of the nervous system. In *British Medical Journal*, volume 2, pages 355–362, 1889.

I. T. Joliffe. *Principal Component Analysis*. Springer Series in Statistics. Springer, 1961.

Ole Kiehn. Locomotor circuits in the mammalian spinal cord. *Annual Review of Neuroscience*, 29:279–306, 2005.

Ole Kiehn, Kimberly J. Dougherty, Martin Hägglund, Lotta Borgius, Adolfo Talpalar, and Carlos Ernesto Restrepo. Probing spinal circuits controlling walking in mammals. *Biochemical and Biophysical Research Communications*, 396:11–18, 2010.

Peter Noble Kugler and Michael T. Turvey. *Information, natural law, and the self-assembly of rhythmic movement*. Lawrence Erlbaum Assoc Inc, 1986.

Mark L. Latash. *Control of human movement*. Human Kinetics, 1993.

Mark L. Latash. *Synergy*. Oxford University Press, USA, 2008.

Mark L. Latash. Motor synergies and the equilibrium-point hypothesis. In Mindy F. Levin, editor, *Motor Control*, volume 14, pages 294–322. Progress in Motor Control, July 2010.

Michael Lewicki and Terrence Sejnowski. Learning overcomplete representations. *Neural Computation*, 12:337–365, 2000.

Stephane Mallat and Zhifeng Zhang. Matching pursuits with time frequency dictionaries. *IEEE Transactions for Signal Processing*, 41(12):3397–3415, 1993.

Mario Manto, james M. Bower, et al. Consensus paper: Roles of the cerebellum in motor control—the diversity of ideas on cerebellar involvement in movement. *Cerebellum*, DOI 10.1007/s12311-011-0331-9, 2011.

PBC Matthews. The dependence of tension upon extension in the stretch reflex of the soleus of the decerebrate cat. In *The Journal of Physiology*, volume 47, pages 521–546, 1959.

F. A. Mussa-Ivaldi, S. Giszter, and E. Bizzi. Linear combinations of primitives in vertebrate motor control. *Proceedings of the National Academy of Sciences USA*, 91(16):7534, 1994.

Jeremy Noble and Stephen Prentice. Adaptation to unilateral change in lower limb mechanical properties during human walking. *Experimental Brain Research*, 169:482–495, 2006.

B. A. Olshausen and D. J. Field. Emergence of simple-cell receptive field properties by learning a sparse code for natural images. *Nature*, 381:607–609, 1996.

B. A. Olshausen and D. J. Field. Sparse coding with an overcomplete basis set: A strategy employed by v1? *Vision Research*, 37:3311–3325, 1997.

David Ostry and Anatol Feldman. A critical evaluation of the force control hypothesis in motor control. *Experimental Brain Research*, 153:275–288, 2003. ISSN 0014-4819.

Emmanuel Pierrot-Deseilligny, Groupe Hospitalier Pitié-Salpétrière, and David Burke. *The Circuitry of the Human Spinal Cord: Its Role in Motor Control and Movement Disorders*. Cambridge University Press, 2005.

Marco Popovic, A. Goswami, and Hugh Herr. Ground reference points in legged locomotion: Definitions, biological trajectories and control implications. In *The International Journal of Robotics Research*, volume 24, pages 1013–1032, 2005.

Marc Raibert. Boston dynamics petman project. URL `www.bostondynamics.com`.

Marc Raibert, Kevin Blankespoor, Gabriel Nelson, and Rob Playter. Bigdog, the rough-terrain quaduped robot. In *IFAC World Congress*, volume 17, 2008.

Rajesh P. N. Rao and Dana H. Ballard. Predictive coding in the visual cortex: a functional interpretation of some extra-classical receptive field effects. *Nature Neuroscience*, 2:79–87, 1998.

S. Schaal. Dynamic movement primitives - a framework for motor control in humans and humanoid robots. *The International Symposium on Adaptive Motion of Animals and Machines.*, 2003.

Terrence Sejnowski. Making smooth moves. *Nature*, 394, 1998.

Luis Sentis, Jaeheung Park, and Oussama Khatib. Compliant control of multi-contact and center of mass behaviors in humanoid robots. *IEEE Transactions in Robotics*, 26(3):483–501, June 2010.

Reza Shadmehr and Sandro Mussa-Ivaldi. *Biological Learning and Control: How the brain builds representations, predicts events, and makes decisions.* MIT Press, 2011.

Elena Yu Shapkova. Spinal locomotor capability revealed by electrical stimulation of the lumbar enlargement in paraplegic patients. In Mark L. Latash and Mindy Levin, editors, *Progress in Motor Control*, volume 3, pages 253–290. Human Kinetics: Champaign, IL, 2004.

C.S Sherrington. Flexion-reflex of the limb, crossed extension reflex, and reflex stepping and standing. *Journal of Physiology*, 40:28–121, 1910.

Evan Smith. *Efficient Auditory Coding.* PhD thesis, Carnegie Mellon University, 2006.

Evan Smith and Michael Lewicki. Efficient auditory coding. *Nature*, 439, 2006.

Emanuel Todorov. Optimality principles in sensorimotor control. *Nature Neuroscience*, 7(9):907–915, 2004.

Emanuel Todorov and Michael Jordan. Optimal feedback control as a theory of motor coordination. *Nature Neuroscience*, 5(11):1226–1225, 2002.

Emanuel Todorov, Weiwei Li, and Xiuchuan Pan. From task parameters to motor synergies: A hierarchical framework for approximately optimal control of redundant manipulators. *J. Robot. Syst.*, 22:691–710, November 2005. ISSN 0741-2223. doi: 10.1002/rob.v22:11. URL `http://dl.acm.org/citation.cfm?id=1093567.1093575`.

Elizabeth B. Torres and David Zipser. Reaching to grasp with a multi-jointed arm. i. computational model. *J Neurophysiol*, 88(5):2355–2367, 2002.

Gerard J. Tortora. *Principles of human anatomy.* Hoboken, NJ : J. Wiley, 10th edition, 2005.

Matthew Tresch and Anthony Jarc. The case for against muscle synergies. *Current opinion in neurobiology*, 2009.

M. T. Turvey. Coordination. *American Psychologist*, 45:938–953, 1990.

Patrick van der Smagt, Markus Grebenstein, Holger Urbanek, Nadine Fligge, Michael Strohmayr, Georg Stillfried, Jonathon Parrish, and Agneta Gustus. Robotics of human movements. *Journal of Physiology - Paris*, pages 119–132, 2009.

Bram Vanderborght. *Dynamic Stabilisation of the Biped Lucy Powered by Actuators with Controllable Stiffness.* PhD thesis, Vrije Universiteit Brussel, 2007.

D. A. Winter. Biomechanics of human movement with applications to the study of human locomotion. In *Critical Reviews of Biomedical Engineering*, volume 9, pages 287–314, 1984.

Solly Zuckerman. *A New System of Anatomy.* Oxford Press, 1961.